Oxidative potential of fine particles at urban and rural sites in eastern and western Japan: Effects of transboundary transport from continental Asia and local emissions

Chiharu Nishita-Hara[1], Kohei Nakano[1], Keiichiro Hara[2], Raga Ishikawa[1], Hiroko Yamanaka[1], Atsushi Matsuki[3], Masahiko Hayashi[2], Tomoaki Okuda[1]

[1] Department of Applied Chemistry, Faculty of Science and Technology, Keio University, Yokohama, 233-8522, Japan
[2] Department of Earth System Science, Faculty of Science, Fukuoka University, Fukuoka, 814-0180, Japan
[3] Institute of Nature and Environmental Technology, Kanazawa University, Kanazawa, 920-1192, Japan

Correspondence to: Chiharu Nishita-Hara (nishitachiharu.z@gmail.com)

Abstract. Oxidative stress is a key mechanism that contributes to the toxicity of atmospheric aerosol particles. We investigated the mass-normalized oxidative potential (OP) of fine particles collected at three sites in Japan: Yokohama (an urban background site in the Greater Tokyo Area), Fukuoka (an urban background site in western Japan), and Noto (a rural site on the Noto Peninsula facing the Sea of Japan). The OP was evaluated using two assays: a cell-free dithiothreitol (DTT) assay (OP_m^{DTT}) and a cell-based assay employing 5-(and-6)-chloromethyl-2',7'-dichlorodihydrofluorescein diacetate, acetyl ester (CM-H_2DCFDA) with alveolar epithelial cells (OP_m^{DCFH}). Both OP metrics exhibited significant spatial variation, with the highest values in Yokohama, followed by those in Fukuoka and Noto. This spatial pattern suggests that fine particles influenced by local urban emissions have higher intrinsic OP than those affected by long-range transport from continental Asia. Secondary particle formation during atmospheric transport likely alters the chemical composition of the particles, providing a plausible explanation for the lower intrinsic OP compared to locally emitted urban aerosol particles. OP_m^{DCFH} was correlated with carbonaceous components derived from fuel combustion and transition metals (Cu, Mn, and Fe) (r = 0.47–0.84), whereas OP_m^{DTT} was associated mainly with the transition metals (r = 0.67–0.82). These results indicate different pathways for reactive oxygen species (ROS) generation in the two assays. Despite these differences, OP_m^{DTT} and OP_m^{DCFH} were positively correlated (r = 0.81), indicating that DTT reactivity can reasonably predict the anthropogenic fine particle-induced increase in intracellular oxidative activity.

1 Introduction

Epidemiological studies have demonstrated associations between exposure to fine particles in the atmosphere and various adverse health outcomes, including increased risks of premature mortality, and of respiratory and cardiovascular diseases (Dockery et al., 1993; Pope et al., 2002; Laden et al., 2006; Hoek et al., 2013; Lelieveld et al., 2015; Cohen et al., 2017; Michikawa et al., 2019). Although the mechanisms underlying of the aerosol particle toxicity have not been fully elucidated, oxidative stress is widely recognized as a major toxicological pathway (Li et al., 2003; Nel, 2005; Xia et al.,

2006; Michael et al., 2013). Oxidative stress refers to a state of imbalance between reactive species including reactive oxygen species (ROS) and antioxidant defenses in biological system, favoring the presence of reactive species. Inhaled aerosol particles can transport ROS such as superoxide radical (O_2^-), hydrogen peroxide (H_2O_2), or hydroxyl radical (·OH) into the respiratory system (Venkatachari et al., 2005), or induce their formation in the respiratory system via redox-active components bounding to aerosol particles (Shiraiwa et al., 2017). Therefore, whereas aerosol particles are currently regulated by mass concentrations, the oxidative potential (OP) of aerosol particles, defined as their capacity to generate ROS or deplete antioxidants, has been proposed as a more health-relevant metric than particle mass (Molina et al., 2020).

To quantify the OP of aerosol particles, various cellular and acellular assays have been used over the years. Among them, the dithiothreitol (DTT) assay, a widely used acellular assay, is favored for its simplicity, low cost, and high reproducibility (Kumagai et al., 2002; Cho et al., 2005; Shiraiwa et al., 2017; Jiang et al., 2019). The assay uses DTT as a surrogate for cellular antioxidants and simulates electron transfer from antioxidants (e.g., nicotinamide adenine dinucleotide phosphate ($NADP^+$) and nicotinamide adenine dinucleotide (NAD^+)) to molecular oxygen (O_2), catalyzed by redox-active components in aerosol particles, leading to the production of O_2^- and H_2O_2 (Li et al., 2009; Jiang et al., 2019). In this assay, DTT is oxidized to its disulfide form. The rate of DTT consumption is used as a proxy for the OP of aerosol particles. One limitation of the DTT assay is its insensitivity to the generation of ·OH, which is the most reactive ROS (Xiong et al., 2017). Another limitation is its inability to capture ROS generated via intracellular metabolic processes involving particle components. For example, polycyclic aromatic hydrocarbons (PAHs), which themselves are not DTT-active (Charrier and Anastasio, 2012), can induce intracellular ROS production through their conversion to quinones via enzymatic pathways involving cytochrome P450-1A1, epoxide hydrolase, and dihydrodiol dehydrogenase (Penning et al., 1999; Jiang et al., 2019). Nevertheless, several epidemiological reports have described that DTT-measured OP exhibits a stronger association with respiratory and cardiovascular outcomes than particle mass (Bates et al., 2019). Pure reagents that have been identified as DTT-active components include water-soluble transition metals (e.g., Cu and Mn; Charrier and Anastasio, 2012), transition metal oxides (Nicolas et al., 2015), and quinones (Kumagai et al., 2002; Charrier and Anastasio, 2012). Other chemical species such as soot-bound quinones (Antiñolo et al., 2015), humic-like substance (HULIS) (Li and Yu, 2011; Verma et al., 2012; Verma et al., 2015), and mineral components (Nishita-Hara et al., 2019; Nishita-Hara et al., 2023) are also suggested to contribute to DTT consumption by aerosol particles.

A cellular assay using 2',7'-dichlorodihydrofluorescein diacetate (DCFH-DA) is also employed widely to assess intracellular ROS production induced by aerosol particles (e.g., Hu et al., 2008; Landreman et al., 2008; Verma et al., 2009; Fushimi et al., 2017; Park et al., 2018a; Al Hanai et al., 2019; Fang et al., 2025). DCFH-DA is a cell membrane-permeable probe that is deacetylated by intracellular esterases to form 2',7'-dichlorodihydrofluorescein (DCFH), a membrane-impermeable and non-fluorescent compound. Then DCFH is oxidized by several ROS to produce the fluorescent product 2',7'-dichlorofluorescein (DCF). Recently, the chloromethyl DCFH-DA (CM-H_2DCFDA) and the carboxylated DCFH-DA (carboxy-H_2DCFDA) have been used as alternative probes (e.g., Liu et al., 2020a; Honda et al., 2023; Jin et al., 2023; Liu et al. 2023). These alternative probes are not direct derivatives of DCFH-DA, but are structurally related compounds intended

to improve intracellular retention and to reduce background fluorescence (Thermo Fisher Scientific, 2025). Although these DCFH-based probes are often assumed to be specific for H_2O_2, that supposition is not accurate. In fact, DCFH-based probes lack specificity for individual reactive species and instead provide a comprehensive assessment of intracellular oxidative activity, including enzyme-mediated, metabolic, and other cellular redox processes (Kalyanaraman et al., 2012; Halliwell and Gutteridge, 2015; Murphy et al., 2022). However, they are sensitive to those generated downstream of H_2O_2 in the ROS generation cascade. The observed fluorescence primarily reflects the oxidative capacity of ROS such as ·OH, peroxynitrite ($ONOO^-$), and peroxyl radical (ROO·) rather than that of H_2O_2 or O_2^- (Halliwell and Gutteridge, 2015; Thermo Fisher Scientific, 2025).

The OP of aerosol particles varies among locations and source environments. OP is commonly expressed as either volume-normalized OP (OP_v), which reflects oxidative capacity per unit air volume, or mass-normalized OP (OP_m), which represents intrinsic oxidative activity per unit particle mass. Because particles from different sources can have substantially different OP_m, OP_v is not necessarily explained by particle mass concentration alone. Previous studies in Europe have shown that secondary inorganic aerosol often accounts for a large fraction of particle mass, whereas DTT-based OP is generally more closely related to traffic-related emissions, biomass burning, and metal-rich sources (Daellenbach et al., 2020; Weber et al., 2021; Borlaza et al., 2022; Dominutti et al., 2023). This source dependence is also supported by a source-specific toxicity study showing relatively high oxidative activity for combustion-derived particles, particularly traffic-related emissions, compared with particles such as ammonium sulfate, ammonium nitrate, and road dust (Park et al., 2018b). In East Asia, DTT-based OP has been examined in relation to source characteristics and spatial variability in urban and source-influenced environments, including sites in Korea and China (Borlaza et al., 2018; Yu et al., 2019; Liu et al., 2020b; Wang et al., 2020; Xing et al., 2023; Cheung et al., 2024; Koo et al., 2025). However, how regional-scale inter-site variations in mass-normalized OP across East Asia are related to local emissions, transboundary transport, chemical composition, and air-mass history remains insufficiently understood.

Aerosol particles in Japan are supplied by local anthropogenic activities and transboundary transport from continental Asia (e.g., Kaneyasu et al., 2014; Shimada et al., 2021; Yoshino et al., 2021). The relative contributions of these sources vary across the country, depending on geographic location and the extent of local urbanization (Yim et al., 2019; Chatani et al., 2020). A Japanese nationwide epidemiological report described a positive association between the mass concentration of fine particles and mortality in eastern Japan, but no clear association in western Japan, suggesting that the toxicity of fine particles might differ among regions within Japan (Michikawa et al., 2019). To elucidate the relationship between oxidative toxicity and emission sources of fine particles in Japan, we evaluated the OP of fine particles collected using a cyclone sampler for approximately one year (May 2022–June 2023) at three sites representing different relative source contributions: Yokohama, Fukuoka, and Noto. We further examined the relationship between OP values measured using the cell-free DTT assay and intracellular ROS production measured using the CM-H_2DCFDA assay.

2 Experiment Methods

2.1 Sampling

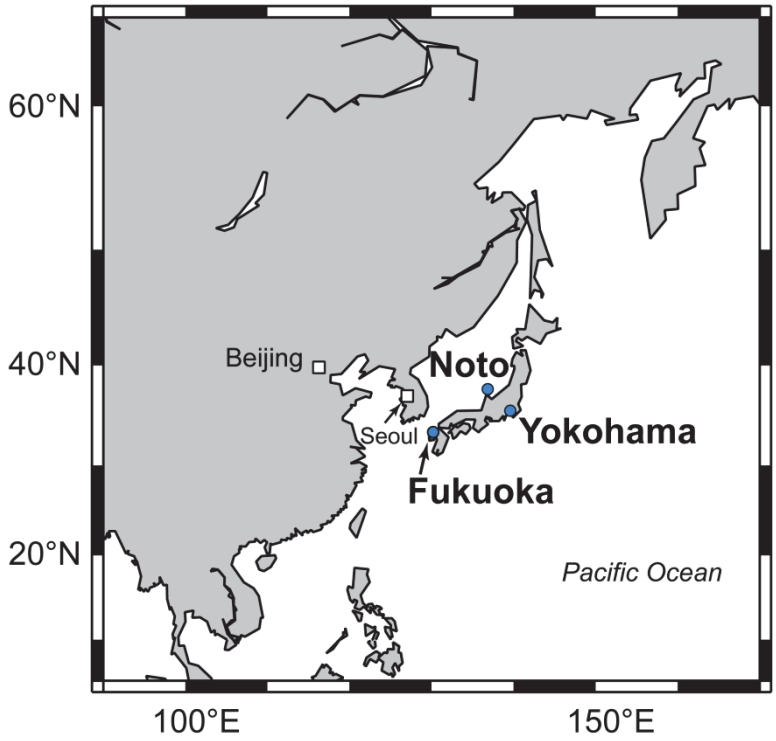

Figure 1. Locations of the Yokohama, Fukuoka, and Noto sampling sites in Japan.

Fine particles were collected at three sites in Japan: Yokohama, Fukuoka, and Noto sites (Figure 1). Yokohama is an urban background site in the Greater Tokyo Area, located at Keio University (35.555°N, 139.655°E) in Yokohama City (Honda et al., 2021). Fukuoka is also an urban background site at Fukuoka University (33.550°N, 130.364°E) in Fukuoka City, a major city in western Japan (Nishita-Hara et al., 2019; Hara et al., 2022). Figure A1 in Appendix A shows land-use and land-cover maps around the sampling sites in 2022, based on a satellite data (High-Resolution Land-Use and Land-Cover Map for Japan, ver. 23.12, https://www.eorc.jaxa.jp/ALOS/en/dataset/lulc/lulc_v2312_e.htm) provided by the Japanese Aerospace Exploration Agency (JAXA). Both the Yokohama and Fukuoka sites are located in typical urban residential areas, approximately 15 km south–southwest of central Tokyo (Tokyo Station) and 5 km southeast of the downtown Fukuoka, respectively. Noto is a rural site located at the tip of the Noto Peninsula, facing the Sea of Japan (Iwamoto et al., 2016). It is situated at the Noto Ground-based Research Observatory (NOTOGRO; 37.451°N, 137.359°E), operated by Kanazawa University. The Noto site is surrounded by the sea, forested areas, and agricultural land, primarily

paddy fields. The nearest major provincial cities to the Noto site are Kanazawa and Toyama Cities, respectively located approximately 115 km to the southwest along the peninsula and 85 km to the south across the sea.

At the three sites, fine particles were collected continuously from May 2022 through June 2023 using a sampling system equipped with a cyclone with a cut-off diameter of 0.2 μm and an impactor functioning as a pre-separator with a cut-off diameter of 2.5 μm (Keio-Transportable Real impactor with Cyclone: K-TRiC), installed on the rooftops of a six-story building at the Yokohama site, a five-story building at the Fukuoka site, and a three-story building at the Noto site. The K-TRiC enables the collection of fine particles with an aerodynamic diameter of 0.2–2.5 μm in powder form. However, not all particles within this size range can be collected because complete recovery of particles captured inside the cyclone is not possible. Therefore, the chemical composition and oxidative potential are reported as mass fractions and mass-normalized values, respectively, rather than as atmospheric (air-volume-based) concentrations. The flow rate of the sampler was maintained at 90 L min^{-1}. The sampling interval was two to three months. Nishita-Hara et al. (2024) provide detailed information related to the K-TRiC. Five samples were collected at both the Yokohama and Fukuoka sites, and four at the Noto site. Table 1 presents the sampling sites, seasons, periods, collected particle masses, and median $PM_{2.5}$ (aerosol particles with a diameter below 2.5 μm) mass concentrations during sampling periods. The median $PM_{2.5}$ mass concentrations were calculated from data obtained at government-managed monitoring stations nearest to each site: the Kohoku-ku Mamedocho station (station code: 14109040), located 4 km south–southwest of the Yokohama site; the Nagao station (station code: 40135020), located 2 km east–northeast of the Fukuoka site; and the Suzu station (station code: 17205020), located 9 km west of the Noto site. The monitoring data were obtained from the National Institute for Environmental Studies, The Environmental Observatory, Air Pollution Monitoring Data File (https://tenbou.nies.go.jp/download/ (accessed 15 Oct. 2025)). The atmospheric $PM_{2.5}$ mass concentrations at Yokohama and Fukuoka were comparable, but were significantly lower in Noto (Table 1).

Table 1. Summary of sampling sites, seasons, periods, collected particle masses, and mean $PM_{2.5}$ mass concentrations in the atmosphere

Sampling	Season	Period	Sample (mg)	Mean $PM_{2.5}$ * ($\mu g\ m^{-3}$)
Yokohama	Early summer	10 May 2022–5 July 2022	30.6	10.2 [6.0]
	Summer	11 July 2022–13 Sep. 2022	24.2	8.8 [5.0]
	Autumn	13 Sep 2022–28 Nov. 2022	41.9	8.7 [4.7]
	Winter	1 Dec. 2022–20 Feb. 2023	50.4	9.7 [7.0]
	Spring	21 Feb. 2023–16 May 2023	95.6	11.3 [6.0]
Fukuoka	Early summer	12 May 2022–13 July 2022	46.9	10.8 [6.4]
	Summer	14 July 2022–26 Sep. 2022	19.1	8.8 [4.7]
	Autumn	26 Sep. 2022–7 Dec. 2022	35.1	9.6 [5.3]
	Winter	7 Dec. 2022–1 Mar. 2023	42.0	11.6 [9.0]
	Spring	3 Mar. 2023–25 May 2023	88.6	14.0 [8.3]
Noto	Summer	26 May 2022–1 Sep. 2022	40.4	5.7 [6.0]
	Autumn	2 Sep. 2022–14 Dec. 2022	33.7	2.4 [5.5]
	Winter	15 Dec. 2022–25 Mar. 2023	41.7	3.2 [6.2]
	Spring	27 Mar. 2023–8 June 2023	52.9	7.1 [5.4]

* The mean $PM_{2.5}$ mass concentrations were calculated from hourly data obtained from the government-managed monitoring stations nearest to each site. Values in square brackets represent the standard deviation.

2.2 DTT and CM-H_2DCFDA assays

The OP of sample particles was assessed using two methods: DTT and CM-H_2DCFDA assays. The DTT assay, a cell-free method, quantifies the OP of aerosol particles based on the depletion of DTT in the sample suspension. The assay was conducted in accordance with the procedures described by Cho et al. (2005), with minor modifications. Briefly, the loss of 100-μM DTT in 0.10 M phosphate buffer (composed of NaH_2PO_4 and K_2HPO_4; pH 7.4) at 37°C was measured. To prepare the sample particle suspension, 2 mg of sample particles were suspended in 19 mL of 0.10 M phosphate buffer. A 1.9 mL aliquot of the particle suspension was mixed with 100 μL of 2 mM DTT solution (final DTT concentration in the reaction mixture = 100 μM) and incubated at 37°C for 6 min in a dry bath incubator (ND-M01; Nissin Rika). Subsequently, 20 μL of 25 mM 5,5-dithiobis-(2-nitrobenzoic acid) (DTNB) was added to the reaction mixture. After centrifugation at 5000 rpm for 5 min, 200 μL of the supernatant was transferred to a 96-well microplate. Residual DTT reacts with DTNB to form 2-nitro-5-thiobenzoic acid (TNB), the concentration of which was found by measuring absorbance at 415 nm using a microplate reader (MPR-A100; AS ONE Corp.). A calibration curve was generated using DTT standard solutions (10, 25, 50,

and 100 μM), which were analyzed in parallel with the samples. A procedural blank was also included. Its DTT consumption was subtracted from that of the samples. The experiment was performed once with three independent replicates (n = 3). The final OP data measured by DTT assay are presented as the DTT loss rate normalized by the particle mass (OP_m^{DTT}) with units of picomole per minute per microgram.

The CM-H_2DCFDA assay quantifies the increase in intracellular ROS production in response to particle exposure using a fluorescent probe, 5-(and-6)-chloromethyl-2',7'-dichlorodihydrofluorescein diacetate acetyl ester (CM-H_2DCFDA; catalog number C6827; Thermo Fisher Scientific), in human alveolar basal epithelial adenocarcinoma cells (A549). The A549 cells were obtained from the Japanese Collection of Research Bioresources (JCRB) Cell Bank, National Institute of Biomedical Innovation, Health and Nutrition. To prepare the particle suspension for exposure, 2 mg of particles were suspended in 20 mL of phenol red-free minimum essential medium (MEM) amino acid solution supplemented with 1% penicillin-streptomycin, yielding a final particle concentration of 100 μg/mL, and the suspension was sonicated for 30 min at 15°C. A549 cells were seeded in black 96-well plates at a density of 100,000 cells/well and were incubated for 24 hr at 37°C in a humidified atmosphere of 5% CO_2. After 24 hr incubation, the cells were incubated with 5 μM CM-H_2DCFDA solution for 30 min to allow intracellular dye uptake. The 5 μM CM-H_2DCFDA solution was prepared by dissolving 50 μg of CM-H_2DCFDA in 17.3 μL of dimethyl sulfoxide with subsequent dilution in 17.3 mL of phenol red-free MEM amino acid solution containing 1% penicillin–streptomycin. After incubation with the dye, cells were washed to remove extracellular CM-H_2DCFDA, and were then exposed to 100 μL of the particle suspension or control medium. Fluorescence intensity was measured at 6 hr post-exposure using an excitation wavelength of 485 nm and an emission wavelength of 530 nm. The results were expressed relative to the fluorescence intensity measured immediately after particle exposure. This normalization reduces well-to-well variability due to differences in probe loading and cell number and minimizes particle-related optical interference such as absorption or scattering of excitation or emission light. OP_m^{DCFH} values were calculated as the fluorescence intensity at 6 hr post-exposure expressed as a percentage of that immediately after exposure. Experiments were conducted twice independently, each with four replicate wells (n = 8 in total).

To assess potential cytotoxicity under the exposure conditions used for the CM-H_2DCFDA assay, including the same cell density, particle concentration, and exposure duration, cell viability was also evaluated using a water-soluble tetrazolium salt-1 (WST-1) assay, which measures mitochondrial metabolic activity in viable cells. The results are presented in Figure A2 in Appendix A. Mean cell viability remained above 80% for all particle samples under the exposure conditions used for the CM-H_2DCFDA assay, suggesting that the contribution of cytotoxic effects to the measured OP_m^{DCFH} values was likely limited. Additionally, to confirm the responsiveness of the CM-H_2DCFDA assay to ROS generation, cells were exposed to hydrogen peroxide (H_2O_2, 100 μM) in combination with iron ions (100 or 200 μM, added as $FeCl_2$), which promote ·OH generation through the Fenton reaction. This treatment resulted in a concentration-dependent increase in fluorescence intensity compared with the control, with the maximum value reaching approximately 300% of the initial value (Figure A3 in Appendix A).

2.3 Airmass backward trajectory analysis

Five-day backward trajectories of air masses arriving at 500 m above ground level at the Yokohama, Fukuoka, and Noto sites during the sampling period were calculated every 6 hr. Calculations were performed using the NOAA HYSPLIT model (Stein et al., 2015) with the GDAS1 meteorological data archive in vertical velocity mode.

2.4 Chemical analysis

The concentrations of water-soluble ions in the sample particles were analyzed using the following procedure. 2 mg of the sample was extracted by shaking it for 15 min in 20 mL of ultrapure water. The concentrations of Cl^-, NO_3^-, SO_4^{2-}, Na^+, NH_4^+, K^+, Mg^{2+}, and Ca^{2+} in the water extracts were measured using ion chromatography (ICS-2100/1100; Thermo Fisher Scientific Inc., Waltham, USA). Analytical conditions of the ion chromatographs were set as described for our earlier work (Nishita-Hara et al., 2024). Concentrations of non-sea-salt (nss) SO_4^{2-}, K^+, Mg^{2+}, and Ca^{2+} were derived from their total concentration using seawater ratios (Seinfeld and Pandis, 2016) and Na^+ concentrations as a sea salt tracer.

The concentrations of carbonaceous components, elemental carbon (EC) and organic carbon (OC), in the sample particles were measured using an ECOC analyzer (Sunset Laboratory Inc.). For analysis of powder-form samples, 300 μg of particles were weighed and deposited onto 10 mm × 10 mm quartz fiber filters (Okuda, 2013). Following the IMPROVE protocol (Chow et al., 1993), OC1–OC4 represent OC fractions volatilized respectively at 120 °C, 250 °C, 450 °C, and 550 °C, under a pure helium atmosphere. EC1–EC3 correspond to EC fractions combusted at 550 °C, 700 °C, and 800 °C, respectively, in a 2% oxygen and 98% helium atmosphere. According to the IMPROVE protocol, pyrolyzed organic carbon (OCP) is defined as the carbon evolved at 550 °C in the oxidizing phase before the OC/EC split point, which is identified as the moment at which the laser reflectance returns to its initial value following the introduction of O_2. However, for this study, because of the non-uniform distribution of sample particles on the filters, the split point could not be identified optically. It was instead fixed at the midpoint between the end of OC4 and the start of EC2.

The concentrations of metals in the sample particles were ascertained using inductively coupled plasma mass spectrometry (ICP-MS, 7700x; Agilent Technologies Inc.). Samples were digested in a modified polytetrafluoroethylene (TFM) container using a microwave-assisted digestion system (Titan MPS; PerkinElmer Inc.) with a mixture of 3 mL hydrofluoric acid (46–51%) and 5 mL nitric acid (96%). Following digestion, the solution was transferred to a perfluoroalkoxy alkane (PFA) beaker evaporated on a hot plate until near solidification to remove hydrofluoric acid. The residue was diluted using nitric acid (4.8%) and an internal standard to a final volume of 20 ml. The concentrations of Mg, Al, K, Ca, Ti, V, Mn, Fe, Cu, Zn, As, Se, and Cd in the solution were quantified using an ICP-MS instrument.

2.5 Statistical analysis

Using analysis of variance (ANOVA) followed by post-hoc multiple comparison tests in R ver. 4.3.1, tests of significance were conducted to evaluate site-to-site differences in the OP values and mass fractions of chemical species.

3 Results and Discussion

3.1 Site-to-site and seasonal variations in the OP_m^{DTT} and OP_m^{DCFH} of fine particles

Figures 2a and 2c respectively present the OP_m^{DTT} and OP_m^{DCFH} values observed for fine particles collected at the Yokohama, Fukuoka, and Noto sites. Figures 2b and 2d show average OP_m^{DTT} and OP_m^{DCFH} values at each site. Both OP metrics differed significantly among the three sites ($p < 0.05$), with the highest values observed at Yokohama and the lowest at Noto. The median (25th–75th percentile) OP_m^{DTT} values were 73 (62–79), 56 (51–60), and 35 (29–48) pmol min^{-1} μg^{-1}, respectively at Yokohama, Fukuoka, and Noto (Figure 2b). Similarly, the median (25th–75th percentile) OP_m^{DCFH} were 236 (227–243), 175 (164–178), and 148 (140–155) %, respectively, at Yokohama, Fukuoka, and Noto (Figure 2d).

The OP_m^{DTT} values observed for the three sites fall within the range described in reports of earlier studies for fine atmospheric aerosol particles (approximately 5–80 pmol min^{-1} μg^{-1}; Shiraiwa et al., 2017). The OP_m^{DTT} values observed at the Fukuoka site in this study were similar to those measured by Nishita-Hara et al. (2019) for fine particles collected at the same site but during a different period, using fundamentally the same DTT assay conditions (measuring the loss of 100 μM DTT in 0.10 M phosphate buffer at pH 7.4; 45 ±11 pmol min^{-1} μg^{-1}). Kurihara et al. (2022) reported mean OP_m^{DTT} values of 14.9 pmol min^{-1} μg^{-1} and 22.6 pmol min^{-1} μg^{-1} for fine particles collected using filters at the Yokohama and Noto sites, respectively, which were significantly lower than our results. The lower OP_m^{DTT} values observed by Kurihara et al. (2022) might have been caused by the lower initial DTT concentration used in their DTT assay (50 μM; Lin and Yu, 2019) and a different extraction method (water suspension extracted from the filter sample by sonication without filtration). The OP_m^{DTT} values for aqueous extracts of fine particles collected at the Fukuoka site were reported by Fujitani et al. (2023), which was much higher (approximately 140–190 pmol min^{-1} μg^{-1}) than the OP_m^{DTT} values observed at the Fukuoka site during this study, which is attributable to the higher pH (8.9) of the buffer solution used in their DTT assay because the DTT consumption rate is highly pH-dependent (Kumagai et al., 2002).

For both OP_m^{DTT} and OP_m^{DCFH}, seasonal variations were smaller than the differences observed among the three sites. Regarding OP_m^{DTT}, the highest values were observed in autumn for all three sites, whereas lower values were generally observed in early summer, summer, or winter (Figure 2a). By contrast, OP_m^{DCFH} exhibited no consistent seasonal pattern across the sites. For example, the highest OP_m^{DCFH} values were observed in summer at Yokohama, in winter at Fukuoka, and in spring at Noto (Figure 2c). The autumn enhancement in OP_m^{DTT} might partly reflect the influence of biomass-burning-related aerosols associated with post-harvest crop residue burning in East Asia. Consistent with this possibility, $nssK^+$ mass fractions were elevated during autumn at all sites, with the highest levels observed in Yokohama and Noto and relatively high levels also observed in Fukuoka (Figure A4 in Appendix A), although the contribution of biomass burning could not be quantitatively evaluated in this study.

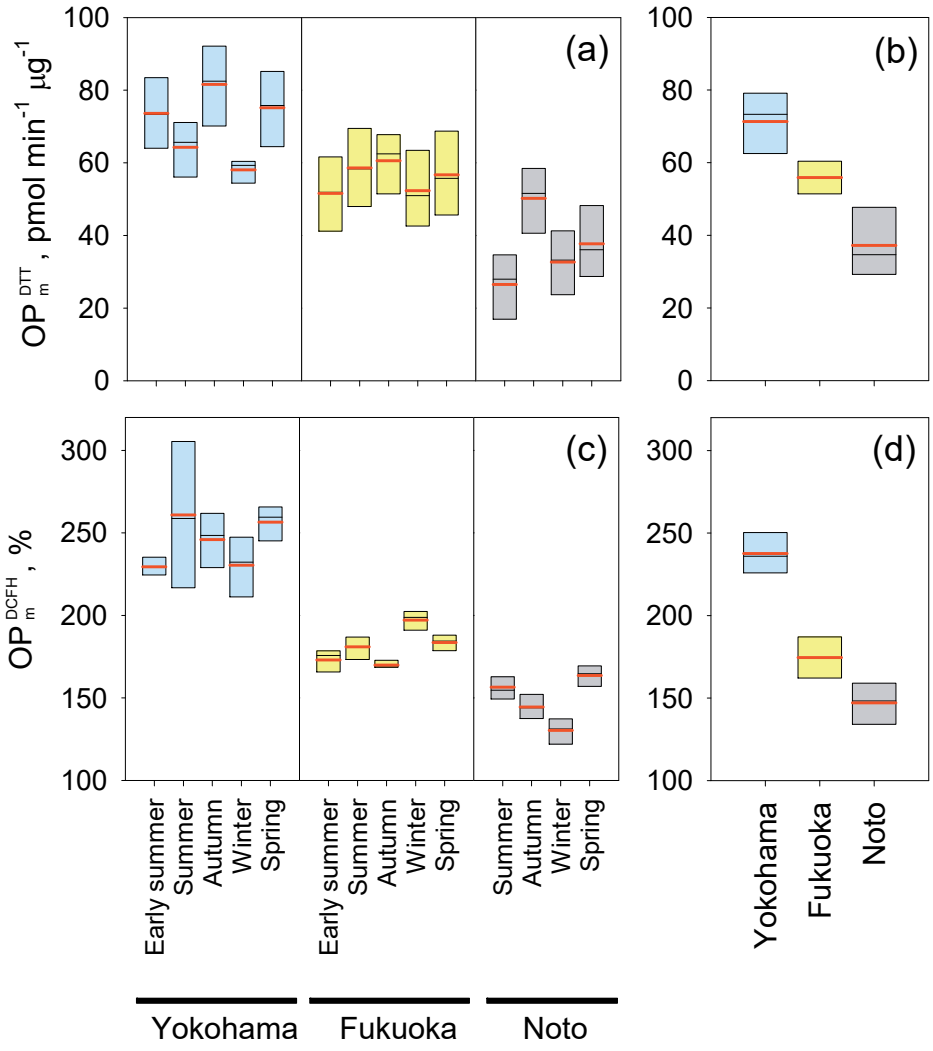

Figure 2. Mass-normalized oxidative potential values of fine particles collected at the Yokohama, Fukuoka, and Noto sites. Panels (a) and (c) show OP_m^{DTT} and OP_m^{DCFH} values for individual samples, respectively. Panels (b) and (d) show the average OP_m^{DTT} and OP_m^{DCFH} values at each site, respectively. In each box plot, the thin black line represents the median, while thick red lines represent the mean. The lower and upper edges of the boxes correspond to the 25th and 75th percentiles, respectively.

Air masses arriving in Japan are transported predominantly by synoptic-scale westerlies, although contributions from the Pacific Ocean increase during summer. Consequently, major sources of atmospheric aerosols in Japan can be categorized broadly into transboundary transport from continental Asia and local anthropogenic emissions near the observation sites. To assess the relative influence of the transboundary transport at the Yokohama, Fukuoka, and Noto sites, we analyzed backward trajectories of air masses during the sampling periods. Figures 3 and 4 respectively portray density maps of 5-day horizontal and vertical backward air-mass trajectories. The vertical trajectories indicate that almost no air masses were transported below an altitude of 2000 m west of longitude 100°E (Figure 4). The fractions of air masses originating from China and Korea were higher at Fukuoka and Noto than at Yokohama (Figure 3), indicating stronger influence from continental Asia at the former two sites. In contrast, local anthropogenic emissions are expected to differ markedly among the sites because of varying levels of urbanization and industrial activity, being highest around Yokohama, and lowest around Noto (Figure A1). Consequently, the relative contribution of local anthropogenic sources to the atmosphere compared to transboundary transport is likely greatest in Yokohama, followed by Fukuoka, and lowest at Noto. Taken together with the observation that OP_m^{DTT} and OP_m^{DCFH} were highest at Yokohama, intermediate at Fukuoka, and lowest at Noto (Figures 2b and 2d), these results suggest that the mass-normalized OP of transboundary-transported fine particles is lower than that of fine particles originating from local emission sources in Japan.

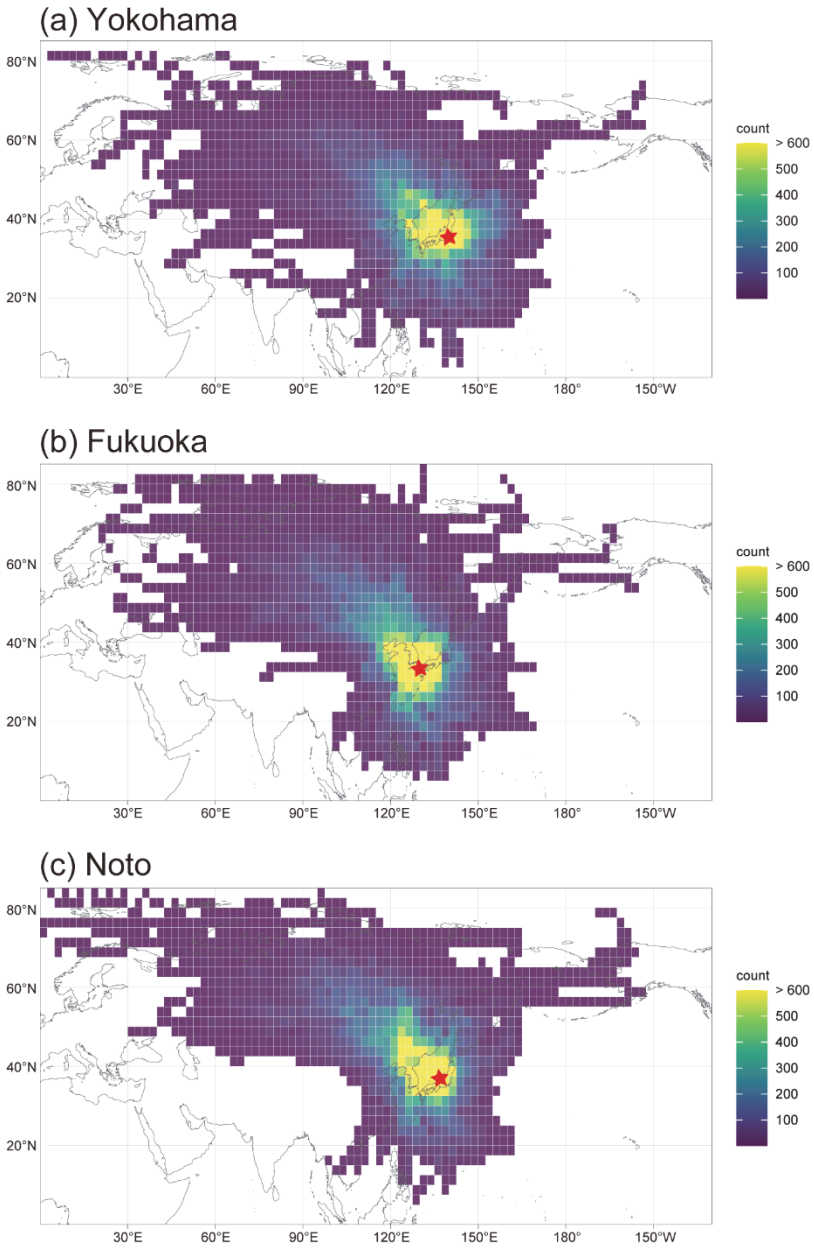

Figure 3. Density maps of 5-day horizontal backward air-mass trajectories calculated for (a) Yokohama, (b) Fukuoka, and (c) Noto during the entire sampling period. Red stars respectively represent the locations of the Yokohama, Fukuoka, and Noto stations in panels (a), (b), and (c).

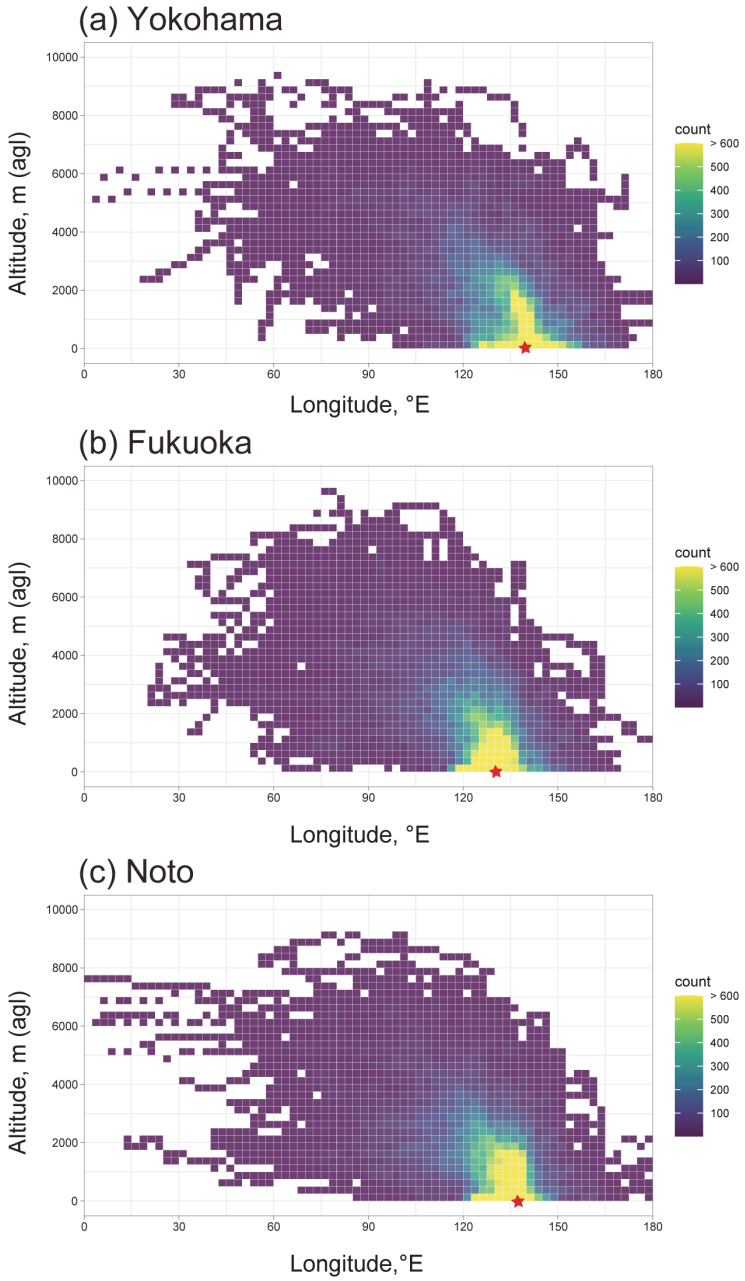

Figure 4. Density maps of 5-day vertical backward air-mass trajectories calculated for (a) Yokohama, (b) Fukuoka, and (c) Noto during the entire sampling period. The trajectories were calculated from an altitude of 500 m above grand level (agl) at each sampling site. Red stars respectively represent the locations of the Yokohama, Fukuoka, and Noto stations in panels (a), (b), and (c).

In contrast to the modest seasonal variations observed in OP_m^{DTT} and OP_m^{DCFH} (Figures 2a and 2c), the seasonal variations in air mass origin were more pronounced than site-to-site differences among the observation sites. Figures 5 and 6 respectively depict density maps of the 5-day horizontal and vertical backward air-mass trajectories arriving at Fukuoka during the respective sampling periods, as examples. The corresponding figures for Yokohama and Noto are shown respectively in Appendix A as Figures A5–A6 and A7–A8. A clear and consistent seasonal transportation pattern was observed across all three sites: air masses originated predominantly from continental Asia in autumn, winter, and spring (Figures 5c, 5d, and 5e), whereas contributions from the Pacific Ocean and domestic sources within Japan increased during summer (Figures 5a and 5b). The limited seasonal variation in OP_m^{DTT} and OP_m^{DCFH} (Figures 2a and 2c), despite the pronounced seasonal changes in air mass transport pathways, can be attributed to seasonal variations in the daytime mixing layer height, which tend to be higher in summer and lower in winter. A higher mixing layer height facilitates the dilution of locally emitted air pollutants, thereby reducing their surface concentrations and their relative contribution to the total particle mass. In fact, in Fukuoka, a summer decrease and a winter increase in the morning and evening maxima of diurnal variations in surface-level atmospheric concentrations of black and organic carbons, NO_x, and CO were observed as associated with seasonal variations in the surface inversion layer (Hara et al., 2022). Consequently, the influence of the seasonal changes in air mass origin on intrinsic OP of fine particles might be counteracted by opposing effects from boundary layer dynamics, consequently leading to smaller seasonal variations in OP_m^{DTT} and OP_m^{DCFH} relative to the differences observed among sites.

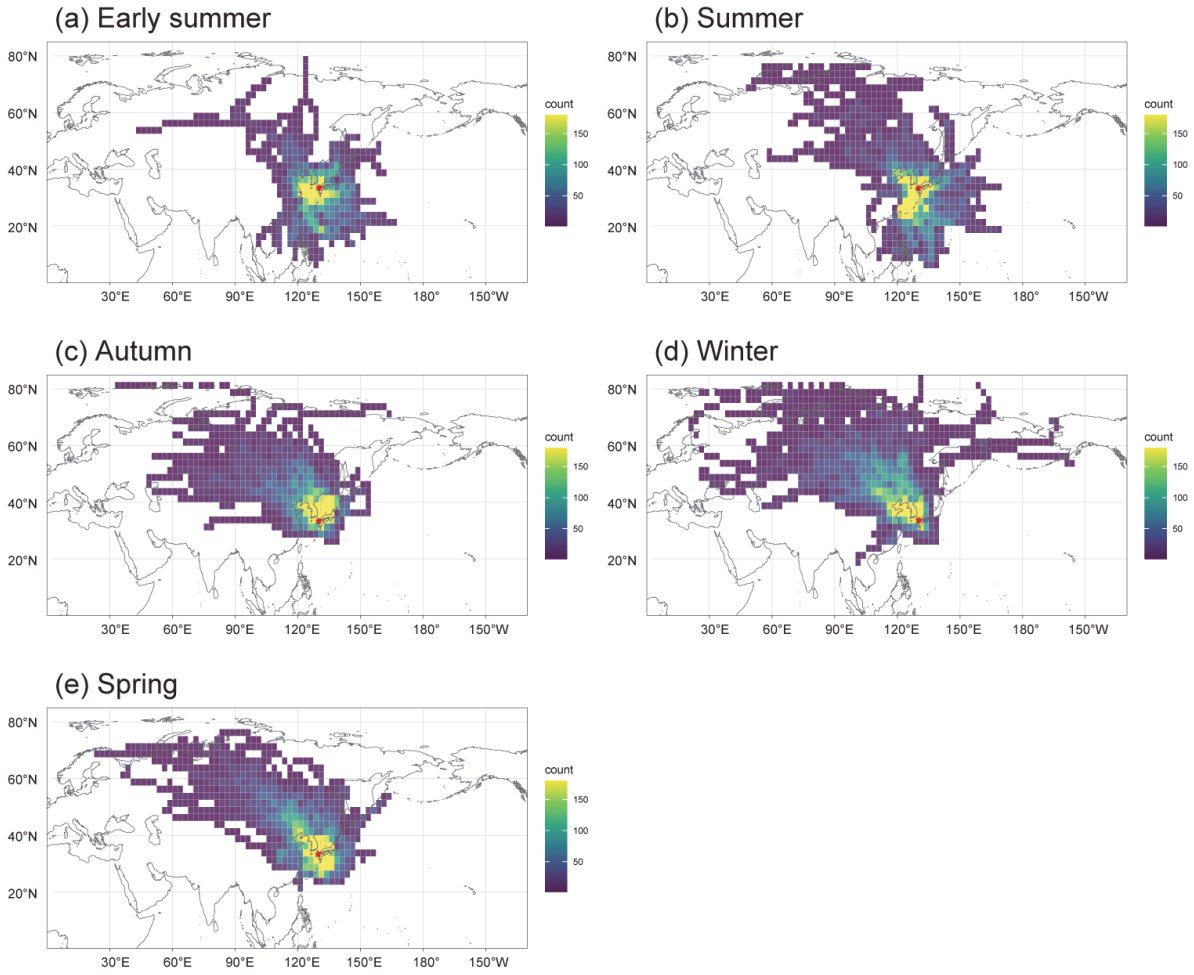

295

Figure 5. Density maps of 5-day horizontal backward air-mass trajectories arriving at Fukuoka during each sampling period: (a) early summer, (b) summer, (c) autumn, (d) winter, and (e) spring. Red stars in each panel denote the location of Fukuoka.

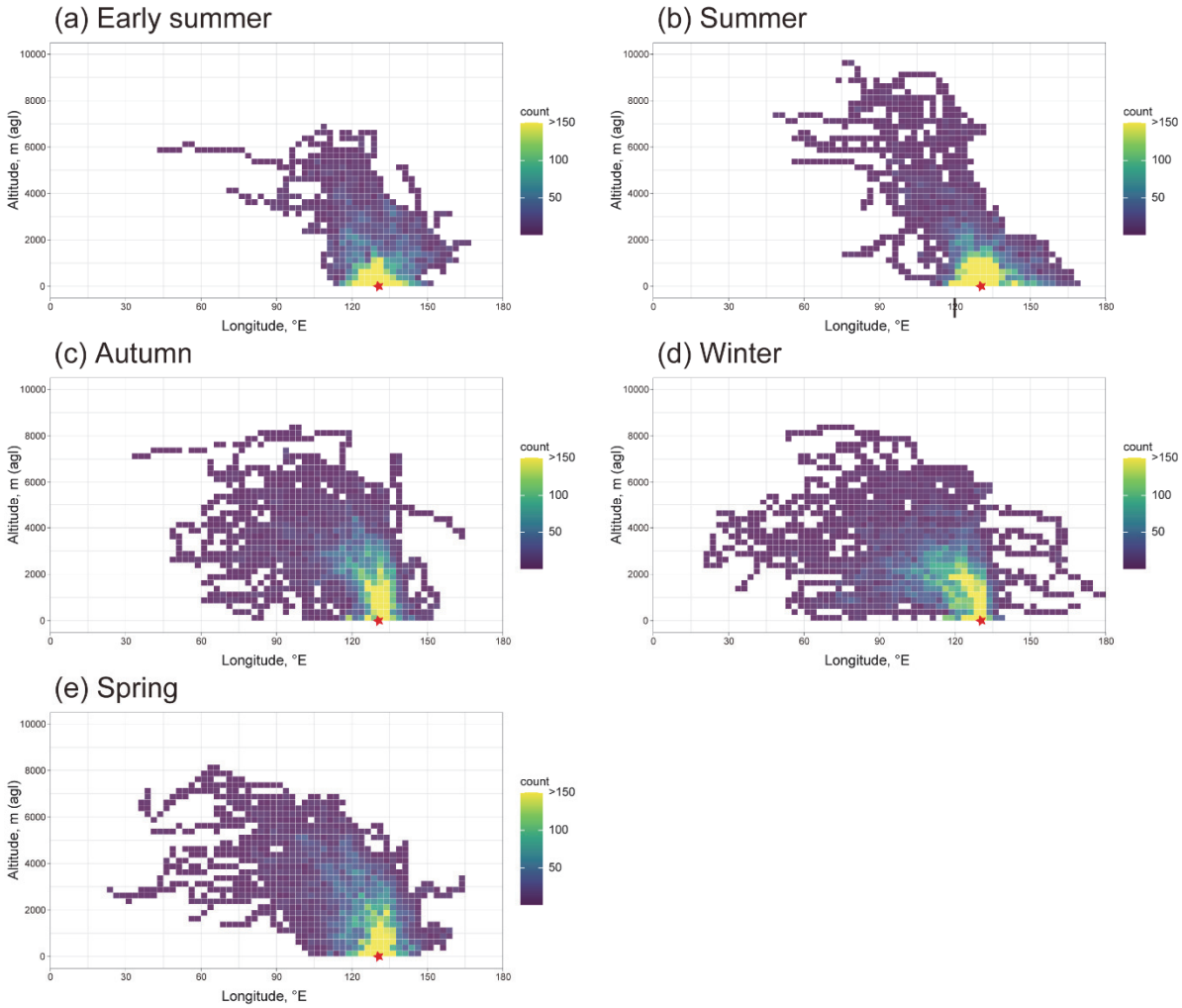

300

Figure 6. Density maps of 5-day vertical backward air-mass trajectories arriving at Fukuoka during each sampling period: (a) early summer, (b) summer, (c) autumn, (d) winter, and (e) spring. Trajectories were calculated from an altitude of 500 m above ground level (agl) at the Fukuoka site. Red stars in each panel denote the location of Fukuoka.

A toxicological study by Onishi et al. (2018) compared the pro-inflammatory response in bronchial epithelial cells (BEAS-2B) after exposure to fine particles collected at Yokohama and Fukuoka: the same sites as those used for this study, but during a different period. They found that pro-inflammatory cytokines, interleukin (IL)-6 and IL-8, were produced at lower levels after exposure to the Fukuoka sample than to the Yokohama sample. Moreover, a Japanese nationwide epidemiological study by Michikawa et al. (2019) reported a positive association between the mass concentration of fine particles and mortality in eastern Japan, but no clear association in western Japan. These findings suggest that fine particles in transboundary-transported aerosols are less toxic than those in locally emitted aerosols in Japan, which is consistent with our results.

3.2 Chemical composition of fine particles and their correlations with OP_m^{DTT} and OP_m^{DCFH}

The mass normalized OP of aerosol particles is presumably governed primarily by their chemical composition, although physical properties might also play a role. Figure 7 presents the chemical composition of fine particles collected at the Yokohama, Fukuoka, and Noto sites. Figures 7a, 7c, and 7e respectively show the mass fractions of water-soluble ions, OC and EC, and metal elements in the sample particles. Figures 7b, 7d, and 7f present the corresponding median mass fraction for each site. Water-soluble ions account for a substantial fraction of the aerosol mass, approximately 23–48%, with SO_4^{2-} and NH_4^+ being the dominant species across all samples (Figure 7a). The mass fraction of NO_3^- remained below 5% in all seasons except winter. In winter, however, the NO_3^- concentration increased to approximately 9% in winter at the Yokohama and Fukuoka sites, while remaining low at the Noto site (< 1.5%). The median total fraction of water-soluble ions was lower at Yokohama than at the other two sites (Figure 7b). OC and EC contributed approximately 9–18% and 1–3% of the particle mass, respectively (Figure 7c). Among OC species, OC2, OC3, and OCP were predominant, whereas EC1 and EC2 were the dominant EC fractions in all samples. The mass fractions of total metal elements were approximately 3–10% (Figure 7e), with Mg, Al, K, Ca, and Fe as the main contributors. The median fraction of total metal elements was highest at Yokohama and lowest at Noto (Figure 7f).

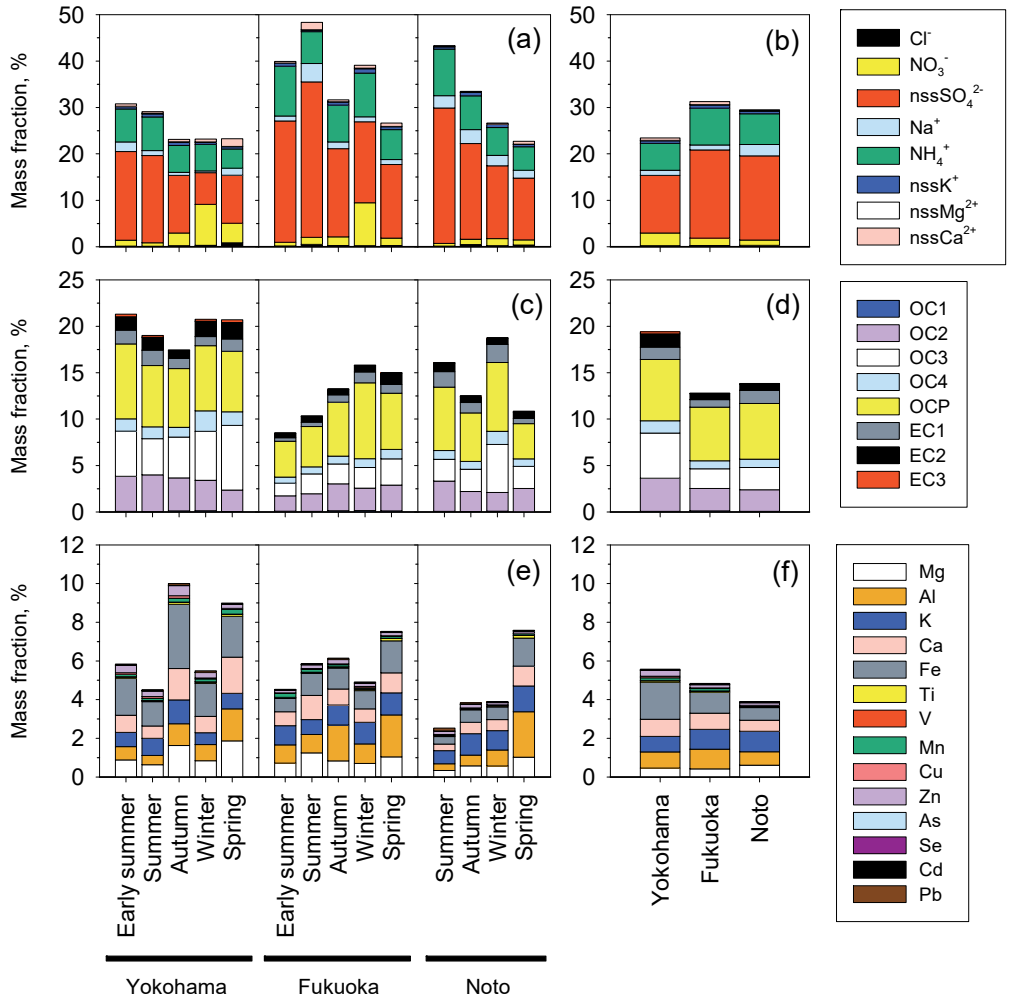

Figure 7. Chemical composition of fine particles collected at the Yokohama, Fukuoka, and Noto sites. Panels (a), (c), and (e) respectively show the mass fractions of (a) water-soluble ions, (c) organic carbon (OC) and elemental carbon (EC), and (e) metal elements in the sample particles. Panels (b), (d), and (f) show the median mass fractions of the corresponding components at the respective sites.

To identify chemical species exhibiting significant site-to-site differences in their mass fractions in fine particles collected at the Yokohama, Fukuoka, and Noto sites, significance tests were conducted. The analyses revealed significant differences for OC2, OC3, OC4, EC2, EC3, Fe, Zn, As, Cu, Mn, and V among the three sites ($p < 0.05$). Figure 8 shows the average mass fractions of these species in the sample particles. Except for As, the mass fractions of these species were significantly higher ($p < 0.05$) in the Yokohama samples compared to those from Noto and/or Fukuoka samples. In contrast, the mass fraction of As was significantly lower at Yokohama site than at the other two sites.

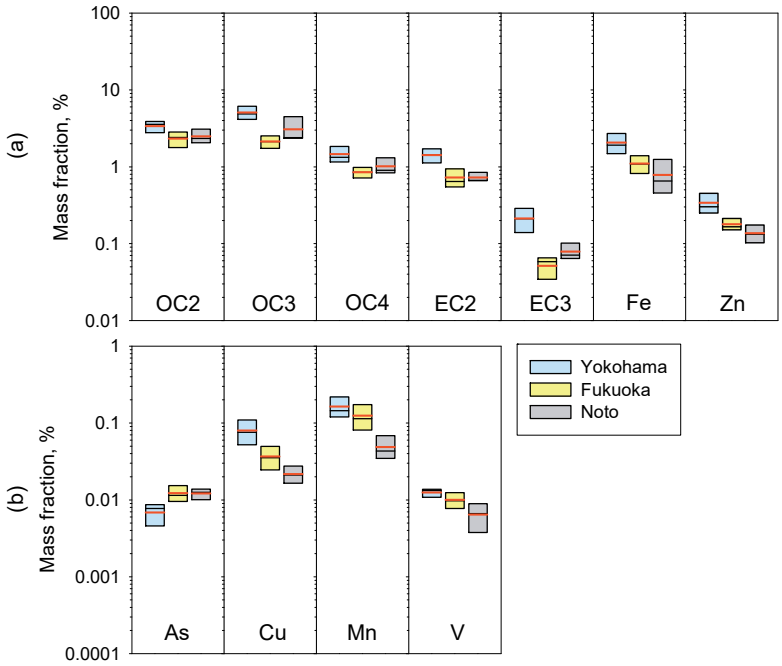

Figure 8. Mass fractions of chemical species that exhibited significant site-to-site differences in fine particles collected at the Yokohama, Fukuoka, Noto sites: (a) OC2, OC3, OC4, EC2, EC3, Fe, and Zn; (b) As, Cu, Mn, and V. In each box plot, the thin black line within the box represents the median value. The thick red line represents the mean value. The bottom and top edges of each box respectively denote the 25th and 75th percentiles.

Figure 9 presents a correlation matrix of the mass fractions of all analyzed chemical species, and OP_m^{DTT} and OP_m^{DCFH} based on hierarchical clustering using the complete linkage method in R (ver. 4.3.1; pheatmap function). According to the cluster analysis of the correlation coefficients, the chemical species, and OP metrics were classified into four groups: Group 1 – Na^+, $nssSO_4^{2-}$, S, $nssK^+$, Cd, NH_4^+, and As; Group 2 – Mg, K, Al, Ti, Cl^-, and $nssCa^{2+}$; Group 3 – OC4, OC3, EC2, EC3, Ca, Mn, V, Fe, OP_m^{DTT}, OP_m^{DCFH}, Cu, and Zn; Group 4 – NO_3^-, OC1, Se, Pb, OCP, EC1, $nssMg^{2+}$, and OC2.

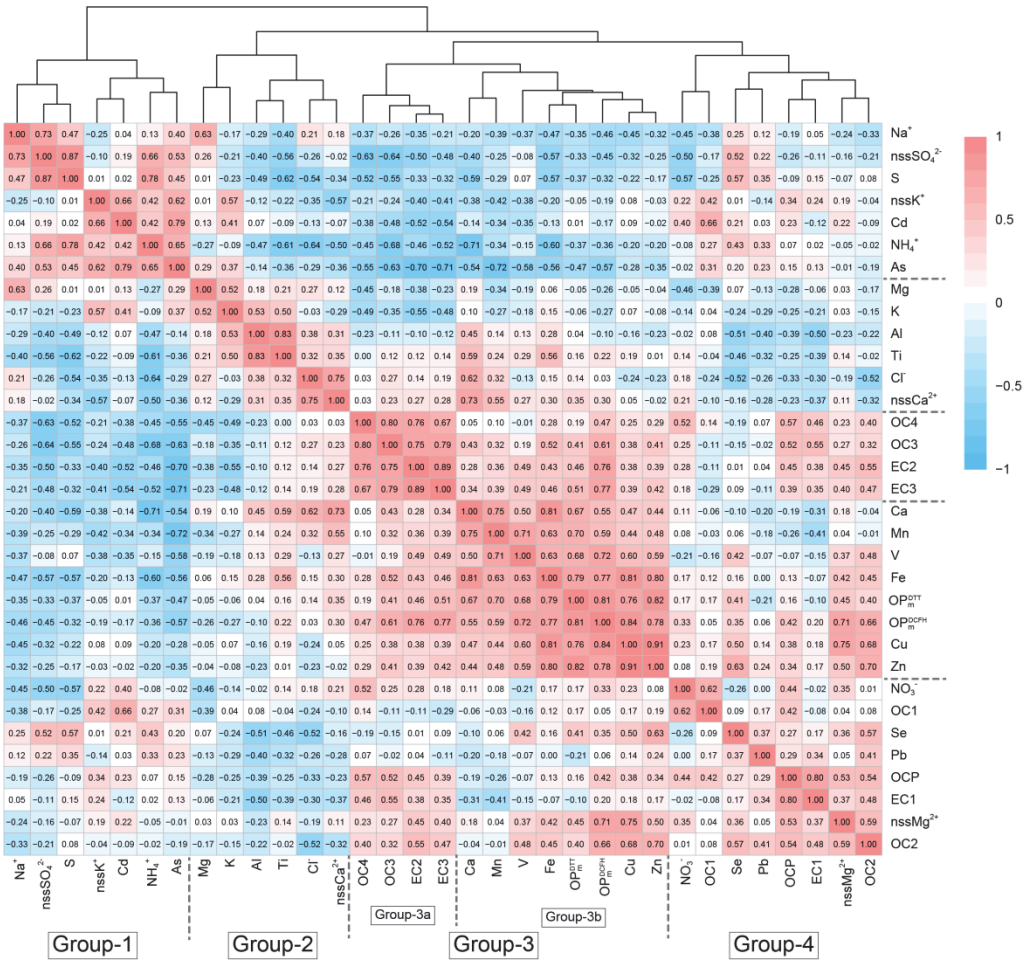

Figure 9. Correlation matrix of the mass fractions of all analyzed chemical species in sample particles, and OP_m^{DTT} and OP_m^{DCFH} with hierarchical clustering. Numbers in the cells represent correlation coefficients. Cells in the correlation matrix are color-coded: red denotes positive correlations; blue represents negative correlations.

Group 1 includes $nssSO_4^{2-}$, As, and $nssK^+$. Sulfate aerosols in East Asia are influenced predominantly by anthropogenic emissions from China (Itahashi et al., 2012). China consumes vast amounts of coal, accounting for approximately half of global coal consumption (Wang and Li, 2016). As in Group 1 is recognized as a typical marker of aerosol particles generated by coal combustion, and atmospheric concentrations in Beijing have been reported to be approximately 20 times higher than those in Tokyo (Okuda et al., 2004). K^+ has also been reported to be emitted in significant amounts from coal combustion in Beijing (Yu et al., 2018). In addition, biomass burning, including agricultural residue burning, is an important source of K^+ in China, particularly during the post-harvest season (e.g., Zhang et al., 2015). Therefore, the sources of the Group 1 species are likely dominated by transboundary transport from China.

Group 2 includes Al and nssCa^{2+}, indicating mineral dust as the primary contributor to the species included in Group 2. In contrast, the mass fractions of all species in Group 3, except for Ca, were significantly higher in the Yokohama samples compared to those from the other sites (Figure 8). Moreover, the Group 3 species exhibited predominantly negative correlations with the Group 1 species (Figure 9). These findings suggest that Group 3 species are associated with local emissions. Group 4 species show positive weak correlations with both Group 1 and Group 3 species (Figure 9), implying that they are influenced both by transboundary transport and by local anthropogenic emissions.

Group 3 can be divided further into two subgroups according to the clustering results: Group 3a (OC3, OC4, EC2, and EC3) and Group 3b (Ca, Mn, V, Fe, OP_m^{DTT}, OP_m^{DCFH}, Cu, and Zn) (Figure 9). Group 3a consists of carbonaceous species typically associated with fuel combustion-derived aerosols, such as vehicular exhaust particles (Cao et al., 2006). OC3 and OC4 are refractory organic compounds, whereas OC1 and OC2 are generally classified as volatile and semi-volatile organic compounds. EC2 and EC3, also known as soot-EC, are formed through gas-to-particle conversion processes at higher combustion temperatures, whereas EC1 is generated mainly by pyrolysis at low combustion temperatures, such as those involved in biomass burning (Han et al., 2007).

Group 3b species comprise metal elements. In urban atmospheres, a wide variety of anthropogenic activities emit metal-containing fine particles. Although the metals in Group 3b were classified into the same group based on clustering analysis, their actual sources might vary widely because of the long sampling periods (2–3 months) in this study. Cu and Zn exhibited a particularly strong correlation ($r = 0.91$), indicating that they might have originated from similar or co-occurring sources. Possible sources of Cu and Zn include fly ash from waste incineration and traffic-related non-exhaust emissions, such as brake wear and tire wear. According to Iijima et al. (2009), Cu/Zn ratios differ markedly between waste fly ash and brake dust (0.07 and 14, respectively). The average Cu/Zn ratio observed in our samples was approximately 0.2, which is closer to that of waste fly ash than to that of brake dust, suggesting that waste fly ash might be an important contributor to Cu and Zn in these samples. However, traffic-related non-exhaust emissions cannot be completely excluded, because this interpretation is based on elemental ratios and clustering analysis rather than formal source apportionment.

It should be noted that the source interpretation in this study was based on chemical composition, hierarchical clustering, and backward trajectory analysis, rather than formal source apportionment such as positive matrix factorization (PMF). Given the limited number of samples (n = 14) and the 2–3 month integration period of each sample, PMF was not expected to provide robust and interpretable source factors for this dataset. Therefore, the inferred relationships between chemical groups and OP should be interpreted qualitatively rather than quantitatively.

Figure 10 presents correlation coefficients of OP_m^{DTT} and OP_m^{DCFH} with the mass fractions of individual chemical species. Both OP metrics exhibited negative correlations with most Group 1 chemical species ($r = -0.57$–0.01), suggesting that the mass-normalized OP of fine particles in Japan tends to decrease as the relative contribution of transboundary transport increases. In Beijing, China, Yu et al. (2019) measured OP_m^{DTT} of the aqueous extract of fine particles collected over the course of one year using the DTT assay under similar conditions to those used in this study: measuring the loss of 100 μM DTT in 0.10 M phosphate buffer at pH 7.4. The mean (standard deviation) OP_m^{DTT} value was 130 (100) pmol min^{-1} μg^{-1},

which was much higher than the values observed in Japan in this study. Therefore, the mass-normalized OP of fine aerosol particles transported from continental Asia might decrease during regional transport to Japan, probably partly because of dilution by secondary particles, such as sulfate, that increase particle mass but do not necessarily contribute proportionally to aerosol OP, consistent with previous source-apportionment studies showing that secondary inorganic aerosol can contribute substantially to particle mass, whereas DTT-based OP is more strongly associated with traffic-related emissions, biomass burning, and metal-rich or mineral-dust-related sources (Weber et al., 2021; Borlaza et al., 2022). Kim et al. (2024) reported a mean (standard deviation) OP_m^{DTT} value of 27.5 (11.8) pmol min^{-1} μg^{-1} for $PM_{2.5}$ collected in Chuncheon, South Korea. Their OP_m^{DTT} value was also determined for particle suspensions including insoluble components, as in the present study, although the comparison should be interpreted with caution because the particles were extracted from filter samples using methanol and might not have been completely recovered from the filters. This value was comparable to the level observed at Noto in this study but lower than those observed at Yokohama and Fukuoka, despite the more urbanized setting of Chuncheon compared with the Noto site. The relatively low OP_m^{DTT} value at Chuncheon might suggest that dilution of redox-active aerosol components had already occurred before or during transport to South Korea.

In contrast to Group 1, Group 2 species showed weak correlations with both OP_m^{DTT} and OP_m^{DCFH} (r=-0.27–0.35), suggesting that the mass-normalized OP of fine mineral dust is comparable with the average mass-normalized OP of fine particles. This finding is consistent with earlier studies conducted at the Fukuoka site (Nishita-Hara et al., 2019; Fujitani et al., 2023), which found that the DTT-measured mass-normalized OP of fine particles during Asian dust events is similar to that on non-event days.

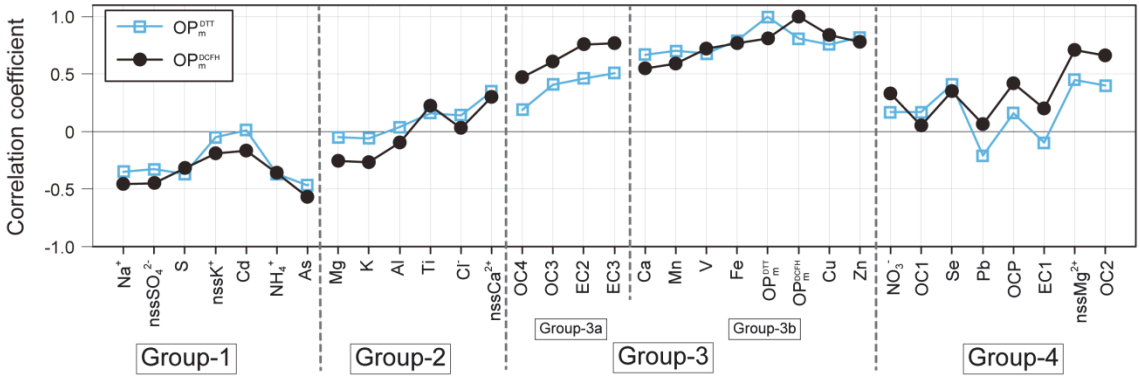

Figure 10. Correlation coefficients of OP_m^{DTT} and OP_m^{DCFH} with the mass fractions of the chemical species.

Most Group 3 species exhibited strong positive correlations with OP_m^{DTT} and OP_m^{DCFH} (r =0.19–0.84), indicating that the mass-normalized OP of fine particles tends to increase with the relative contribution of local sources (Figure 10). The correlation coefficients of OP_m^{DCFH} with Group 3a species (r = 0.47–0.77) were higher than those of OP_m^{DTT} with the same group of chemical species (r = 0.19–0.49) (Figure 8). This discrepancy might be attributed to the intracellular ROS generation that cannot be captured by DTT assay. As discussed above, Group 3a species are primarily associated with

aerosols originating from fuel combustion. Therefore, it is likely that fine particles derived from fuel combustion contain chemical components that contribute substantially to intracellular ROS generation but not to DTT consumption. Candidates as such chemical components are PAHs. Although PAHs do not contribute DTT consumption in the DTT assay (Charrier and Anastasio, 2012), intracellular metabolic products of PAHs (e.g., quinones) are known to enhance intracellular ROS production (Penning et al., 1999).

Both OP_m^{DCFH} and OP_m^{DTT} exhibited strong positive correlations with the mass fractions of Group-3b transition metals (Mn, V, Fe, Cu and Zn) (r = 0.67–0.81). According to Charrier and Anastasio (2012), the DTT reactivity of water-soluble transition metals follows the order of Cu (II) > Mn (II) >> V (III) > Fe (II) > Fe (III), whereas the DTT consumption by water-soluble Zn (II) is negligibly low. After Nicolas et al. (2015) evaluated the DTT reactivity of metal oxide nanoparticles, including CuO, MnO_2, and ZnO, they reported surface-area-normalized reactivity in the order of CuO > MnO_2 >> ZnO. In our samples, the concentrations of these transition metals followed the order of Fe >> Zn >> Mn > Cu >>V (Figure 8). Considering both the intrinsic DTT reactivities of each metal and measured elemental concentrations of the transition metals, Cu and Mn are likely to be significant contributors to OP_m^{DTT} because of their high intrinsic DTT reactivity. Although water-soluble Fe exhibits low reactivity in the DTT assay, its high mass fraction suggests that it might still contribute considerably to OP_m^{DTT}. The strong correlations observed between OP_m^{DCFH} and Group 3b transition metals indicate that they play a major role also in intercellular ROS formation.

Figure 11 portrays a scatter plot comparing the observed OP_m^{DTT} and OP_m^{DCFH} values. As discussed above, the sources of aerosol particles contributing to OP_m^{DTT} and OP_m^{DCFH} can be regarded as not completely identical (Figure 10). Nevertheless, a strong correlation was found between the two OP metrics when data from all sampling sites were combined (r = 0.81), suggesting that the increase in intracellular oxidative ability induced by fine particle exposure can be predicted to some extent from their DTT reactivity in Japan. This overall correlation might be associated with the positive correlation between Group 3a and Group 3b species (Figure 9), both of which are influenced strongly by local emissions. However, Figure 11 also indicates that the relationship between OP_m^{DTT} and OP_m^{DCFH} was less apparent within individual sites, suggesting that the overall correlation was influenced primarily by differences among sites rather than by consistent seasonal covariation within each site. A clear correlation between the two metrics might be detectable only when the dataset covers a sufficiently wide range of OP values.

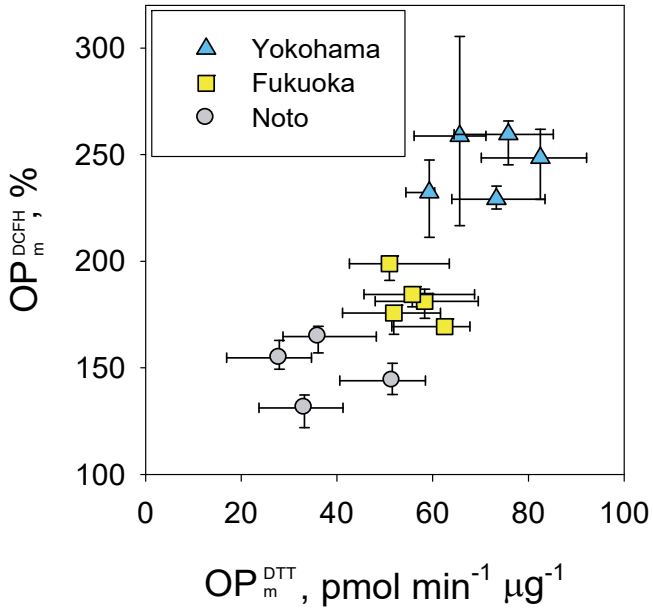

Figure 11. Comparison of OP_m^{DTT} and OP_m^{DCFH} values. Error bars represent the 25th and 75th percentiles of replicate measurements.

Similar to our study, Al Hanai et al. (2019) compared OP values obtained using both the DTT assay and the DCFH-DA assay with rat alveolar macrophages for fine particles collected in Tehran, Iran, an urban area influenced by both mineral dust and local anthropogenic emissions. They reported a significant positive correlation between the two OP metrics (r = 0.73). Similarly, Hu et al. (2008) evaluated OP values using both assays with rat alveolar macrophages for fine particles collected at five sites in Los Angeles, USA, and observed a comparable correlation (r = 0.78). By contrast, no significant correlation was found between the OP values measured by the two assays for fine particles collected during a wildfire event in Los Angeles, likely because of the presence of polar organic compounds in woodsmoke, which contribute to DTT consumption but which induce low levels of intracellular ROS production as measured by the DCFH-DA assay (Verma et al., 2009). However, for fine particles emitted from the open burning of cereal straw and rice husk, a strong correlation (r = 0.80) between OP values measured using the DTT and DCFH-DA assays was reported (Fushimi et al., 2017). When OP data from aerosols that are strongly influenced by biomass burning and mainly influenced by anthropogenic air pollution are included in the same dataset, the correlation between OP values measured using the two assays might deteriorate. Unlike our study, those earlier studies analyzed water suspensions or aqueous extracts of aerosol particles collected on filters, used the conventional DCFH-DA probe rather than CM-H_2DCFDA, and employed rat alveolar macrophages instead of A549 cells. Therefore, direct comparison of correlation coefficients among studies should be interpreted with caution, and the specific factors influencing OP values observed in those studies might differ from ours. Nonetheless, these previous findings,

together with the significant overall correlation observed in the present study, suggest that the two assays can respond similarly to differences in aerosol oxidative properties associated with anthropogenic emissions.

4 Conclusions

This study investigated the mass-normalized OP of fine particles collected at three sites in Japan: an urban background site in the Greater Tokyo Area (Yokohama), an urban background site in a major city in western Japan (Fukuoka), and a rural site on the Noto Peninsula (Noto). The mass-normalized OP was analyzed using two assays: an in vitro alveolar epithelial cell-based CM-H_2DCFDA assay (OP_m^{DCFH}) and a cell-free DTT assay (OP_m^{DTT}). Both OP_m^{DCFH} and OP_m^{DTT} showed significant differences among the sites, with the highest values observed in Yokohama, followed by Fukuoka and Noto. This spatial pattern suggests that fine particles transported from continental Asia exhibit lower intrinsic OP than those emitted from domestic sources in Japan. Secondary particle formation, such as sulfate, during atmospheric transport from the continent likely dilutes the OP-active components, leading to a lower mass-normalized OP for long-range transported fine particles. Results show that OP_m^{DCFH} was correlated positively with the mass fractions of carbonaceous species derived from fuel combustion and with transition metals such as Cu, Mn, and Fe. By contrast, OP_m^{DTT} was found to have strong correlation with the transition metals but weaker correlation with the carbonaceous species. This difference indicates that the chemical species contributing to each OP metric are not completely identical, and that intracellular ROS production, which cannot be captured by DTT assay, might occur via cellular metabolic processes of the chemical components derived from fuel combustion, such as PAHs, and might contribute strongly to intracellular production of ROS. Despite these mechanistic differences, OP_m^{DCFH} and OP_m^{DTT} were found to be strongly correlated ($r = 0.81$), likely because of positive correlations between the fossil fuel combustion-derived particles and transition metal containing particles, both of which are influenced strongly by local anthropogenic emissions in Japan. The correlation suggests that the increase in intracellular oxidative activity induced by exposure to atmospheric fine particles dominated by anthropogenic sources can be reasonably predicted from their DTT reactivity measured in a cell-free system.

Appendix A

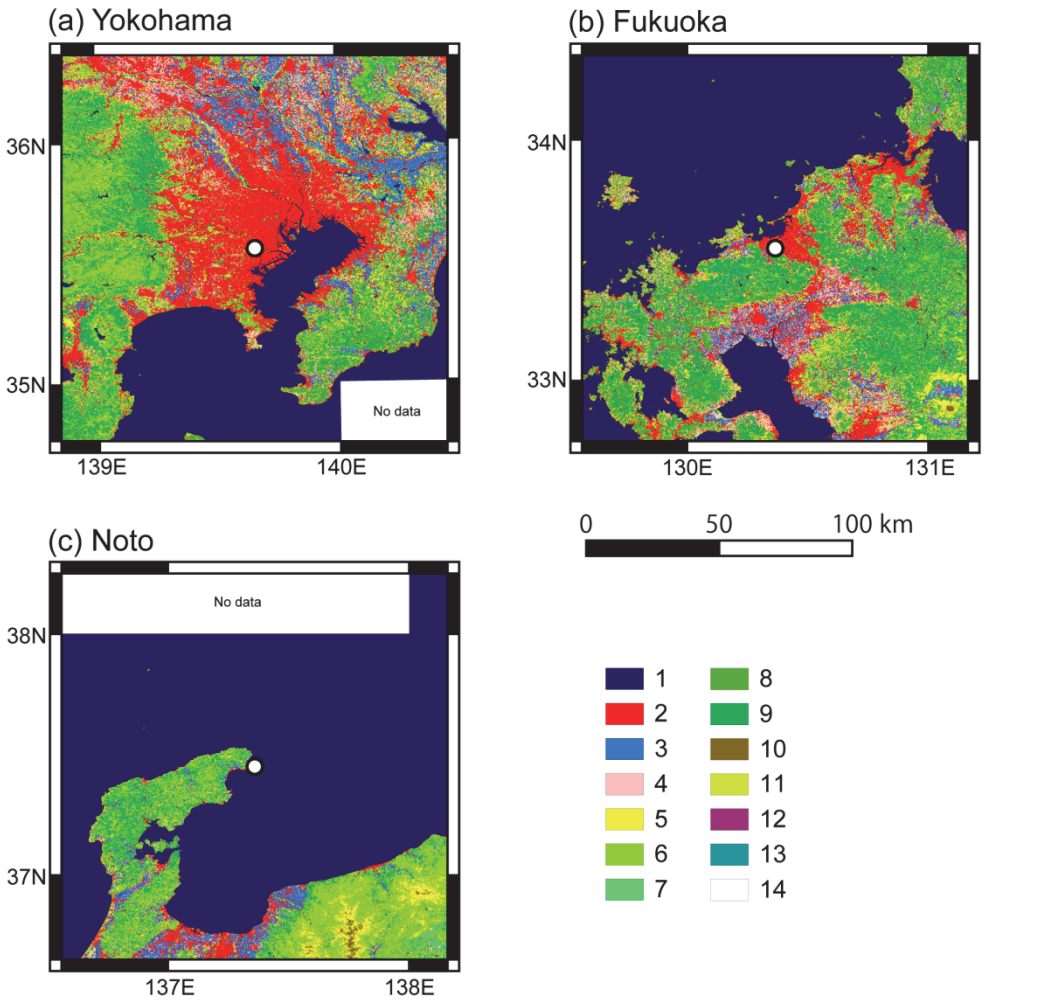

Figure A1. Land-use and land-cover maps around the sampling sites: (a) Yokohama, (b) Fukuoka, and (c) Noto. White circles in each panel denote the locations of the sampling sites. Colored tiles represent the following categories: 1, Water bodies; 2, Built-up; 3, Paddy field; 4, Cropland; 5, Grassland; 6, Deciduous broad-leaved forest (DBF); 7, Deciduous needle-leaved forest (DNF); 8, Evergreen broad-leaved forest (EBF); 9, Evergreen needle-leaved forest (ENF); 10, Bare land; 11, Bamboo forest; 12, Solar panel; 13, Wetland; and 14, Greenhouse. Data are based on the JAXA High-Resolution Land-Use and Land-Cover Map of Japan for 2022, released in December 2023 (Version 23.12; https://www.eorc.jaxa.jp/ALOS/en/dataset/lulc/lulc_v2312_e.htm)

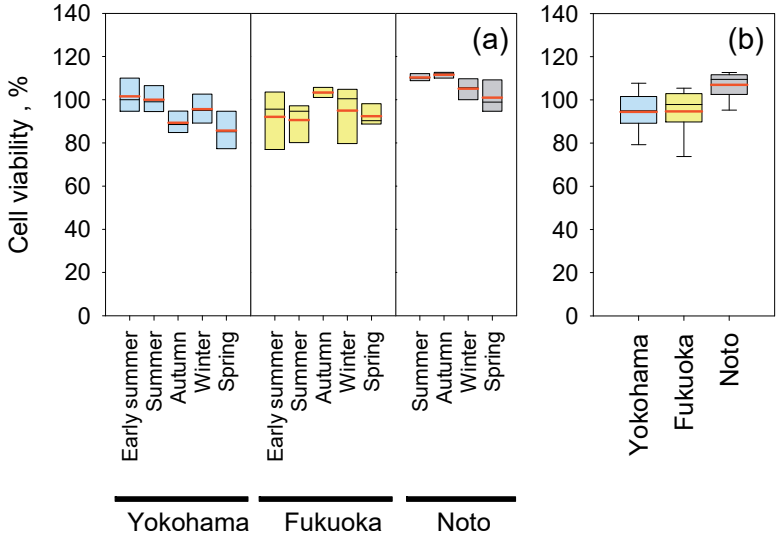

Figure A2. Cell viability of A549 cells exposed to particle suspensions under the same conditions used for the CM-H_2DCFDA assay. Cell viability was evaluated using the WST-1 assay after 6 hr exposure to particles at a concentration of 100 µg/mL. Values are expressed relative to the control. (a) Mean cell viability for individual particle samples based on four independent measurements. (b) Mean cell viability grouped by sampling location. The thin black line represents the median, while thick red lines represent the mean. The lower and upper edges of the boxes correspond to the 25th and 75th percentiles, respectively.

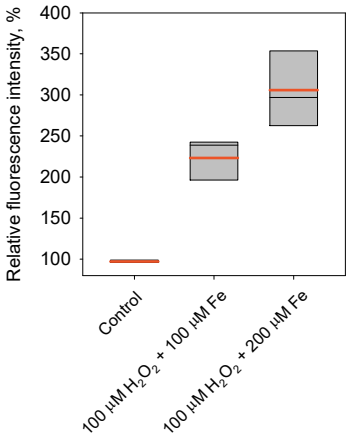

510

Figure A3. Responsiveness of the CM-H₂DCFDA assay in A549 cells to H_2O_2 (100 µM) with iron ions (100 or 200 µM as $FeCl_2$). Control samples are shown for comparison. Data are based on five independent measurements. The thin black line represents the median, while thick red lines represent the mean. The lower and upper edges of the boxes correspond to the 25th and 75th percentiles, respectively.

515

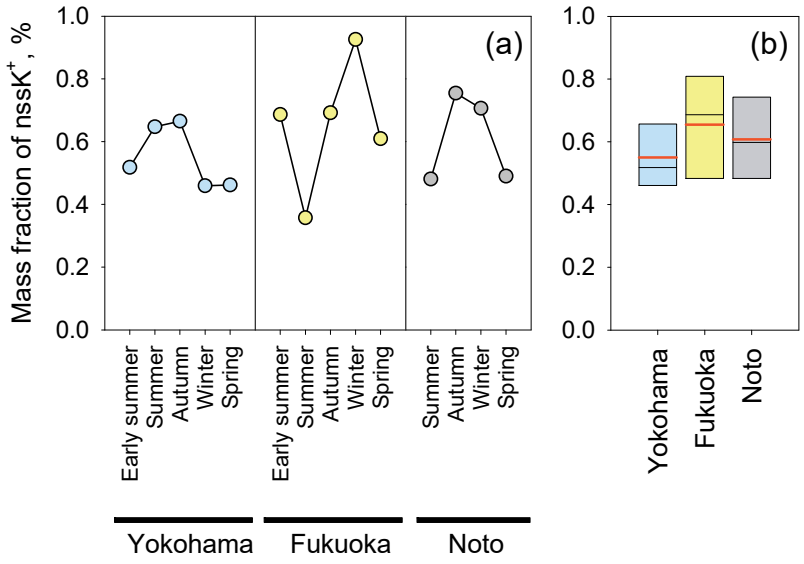

Figure A4. Mass fraction of nssK$^+$: (a) mass fractions for individual particle samples and (b) mean values for the Yokohama, Fukuoka, and Noto sites. The thin black line represents the median, while thick red lines represent the mean. The lower and upper edges of the boxes correspond to the 25th and 75th percentiles, respectively.

520

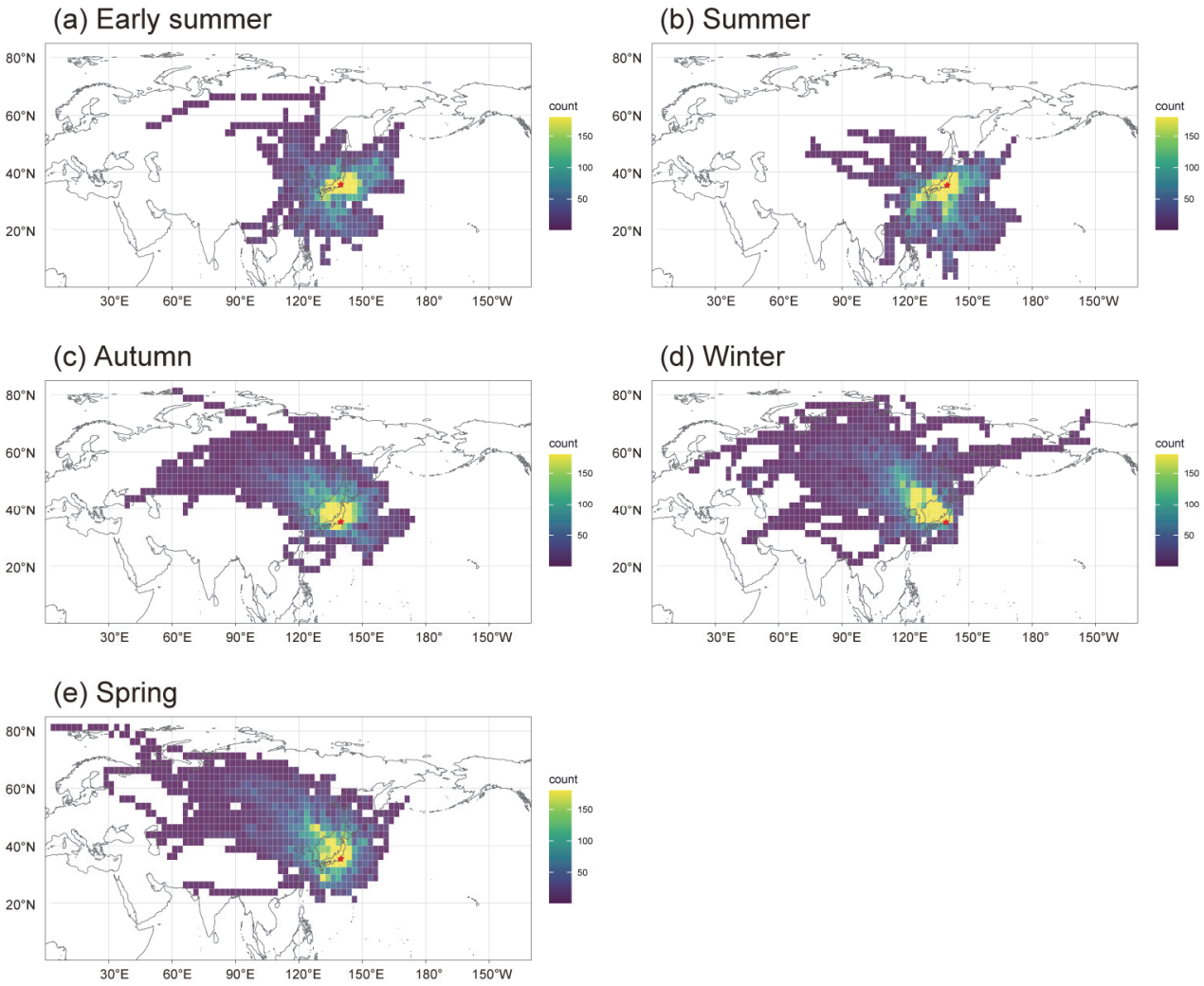

Figure A5. Density maps of 5-day horizontal backward air-mass trajectories arriving at Yokohama during each sampling period: (a) early summer, (b) summer, (c) autumn, (d) winter, and (e) spring. Red stars in each panel represent the location of Yokohama.

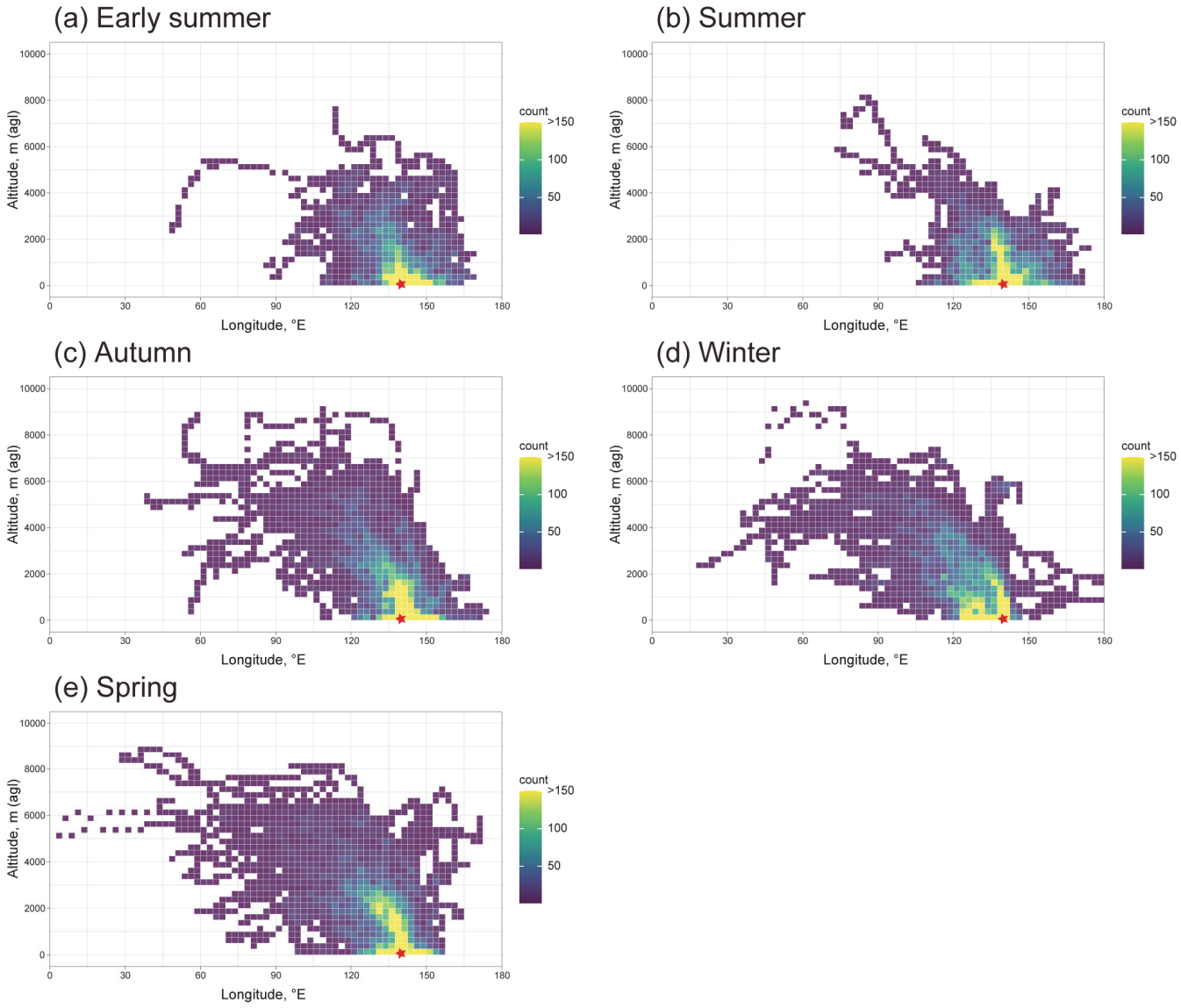

Figure A6. Density maps of 5-day vertical backward air-mass trajectories arriving at Yokohama during each sampling period: (a) early summer, (b) summer, (c) autumn, (d) winter, and (e) spring. Red stars in each panel represent the location of Yokohama.

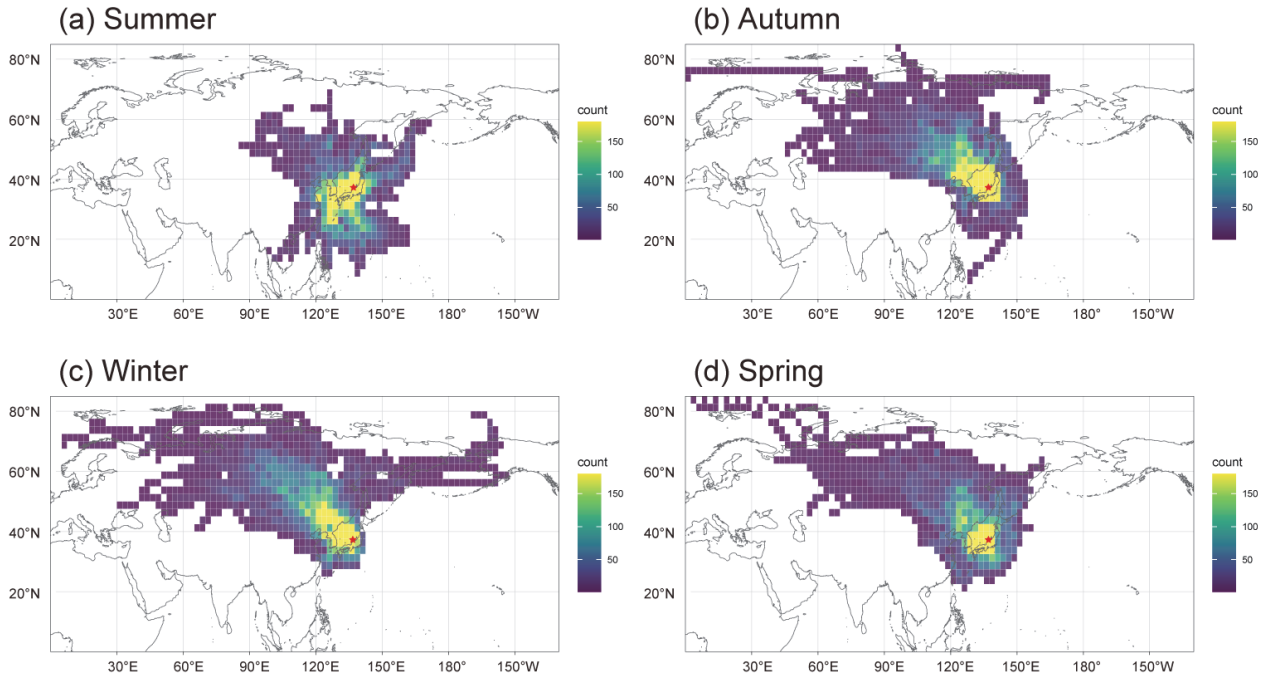

Figure A7. Density maps of 5-day horizontal backward air-mass trajectories arriving at Noto during each sampling period: (a) summer, (b) autumn, (c) winter, and (d) spring. Red stars in each panel represent the location of Noto.

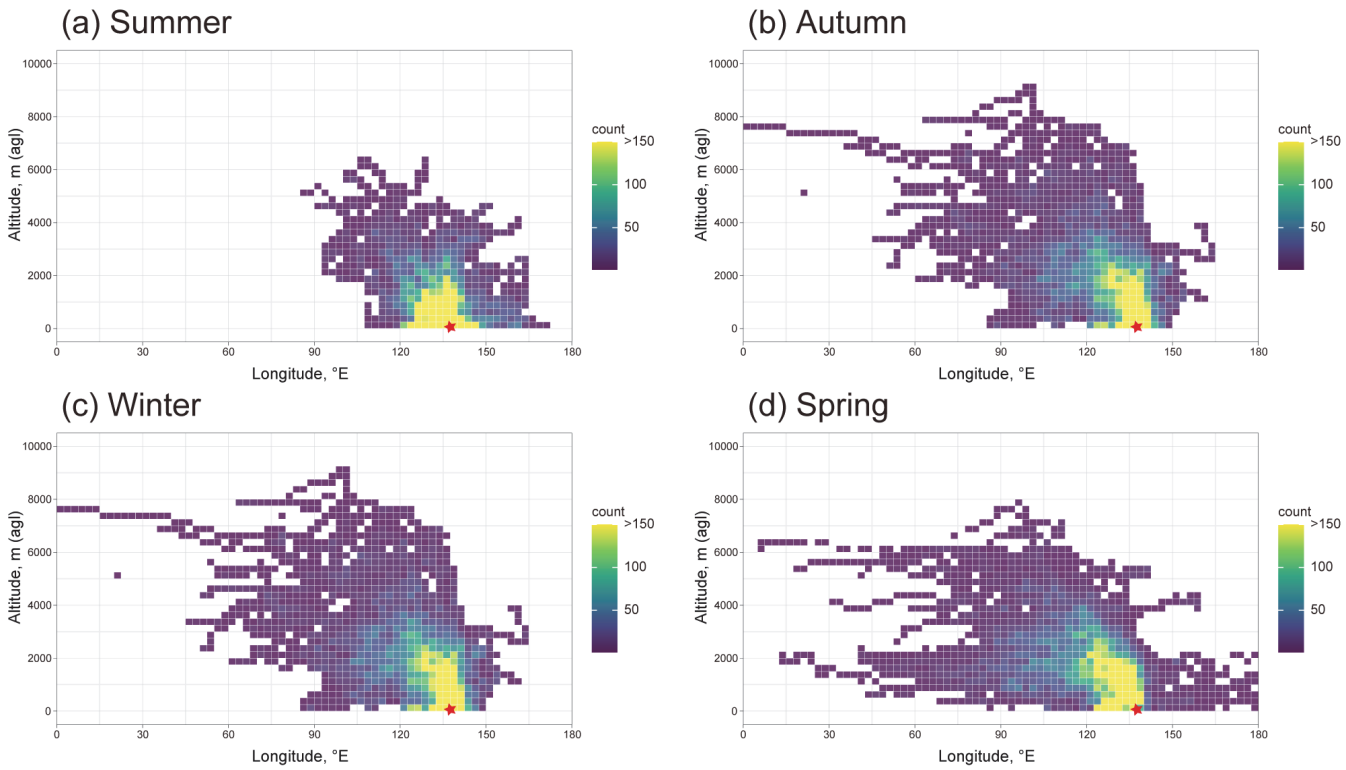

Figure A8. Density maps of 5-day vertical backward air-mass trajectories arriving at Noto during each sampling period: (a) summer, (b) autumn, (c) winter, and (d) spring. Red stars in each panel represent the location of Noto.

Data availability

Observational data are available from the corresponding author upon request.

Author contributions

CNH: Formal analysis, Investigation, Writing – Original Draft. **KN**: Conceptualization, Methodology, Formal analysis, Investigation, Writing – Original Draft. **KH:** Investigation, Resources, Writing – Review and Editing. **RI:** Investigation, Writing – Review and Editing. **HY:** Investigation, Writing – Review and Editing. **AM:** Resources, Writing – Review and Editing. **MH:** Resources, Writing – Review and Editing. **TO:** Conceptualization, Methodology, Writing – Review and Editing, Project administration, Funding acquisition.

Disclosure statements

The authors declare that they have no conflict of interest.

Acknowledgements

The authors are grateful to Akiko Honda for her valuable advice about biological experiments, to Tatsuhiro Mori, Tomoki Sugioka, Hiroaki Tonai, Hina Nagayama, Shoya Manabe, and Ryuki Kato for their assistance with sample collection, chemical analysis, and biological experiments, to Tokyo Dylec Corp. for granting access to the ECOC analyzer, and to Liu Yang for her assistance with the ECOC measurements. We acknowledge the use of ChatGPT (OpenAI) to assist with improving the clarity and grammar of parts of the manuscript. All scientific interpretations, results, and the final text were reviewed and approved by the authors. The authors would like to express their deepest sympathy to residents of Noto, one of the sampling sites in this study, which was damaged severely by the January 2024 earthquake.

Financial support

This work was supported by JST CREST (JPMJCR19H3), the Environmental Research and Technology Development Fund of the Environmental Restoration and Conservation Agency (ERCA) (JPMEERF20165051 and JPMEERF20205007), JSPS KAKENHI Grant Numbers JP22K19851, JP23H03149, JP23KK0195, JP23K27839, JP24K02684, JP24K13416, JP24K03068, JP25K22860, and JP26K15196, the Keio Leading-edge Laboratory Science and Technology Specified Research Projects, the Amano Institute of Technology, and the cooperative research program of the Institute of Nature and Environmental Technology, Kanazawa University (No. 22055 and 23046).

References

Al Hanai, A. H., Antkiewicz, D. S., Hemming, J. D. C., Shafer, M. M., Lai, A. M., Arhami, M., Hosseini, V., and Schauer, J. J.: Seasonal variations in the oxidative stress and inflammatory potential of PM in Tehran using an alveolar macrophage model: The role of chemical composition and sources, Environ. Int., 123, 417–427, https://doi.org/10.1016/j.envint.2018.12.023, 2019.

Antiñolo, M., Willis, M. D., Zhou, S., and Abbatt, J. P. D.: Connecting the oxidation of soot to its redox cycling abilities, Nat. Commun., 6, 6812, https://doi.org/10.1038/ncomms7812, 2015.

Bates, J. T., Fang, T., Verma, V., Zeng, L., Weber, R. J., Tolbert, P. E., Abrams, J. Y., Sarnat, S. E., Klein, M., Mulholland, J. A., and Russell, A. G.: Review of acellular assays of ambient particulate matter oxidative potential: Methods and relationships with composition, sources, and health effects, Environ. Sci. Technol., 53, 4003–4019, https://doi.org/10.1021/acs.est.8b03430, 2019.

Borlaza, L. J. S., Cosep, E. M. R., Kim, S., Lee, K., Joo, H., Park, M., Bate, D., Cayetano, M. G., and Park, K.: Oxidative potential of fine ambient particles in various environments, Environ. Pollut., 243, 1679–1688, https://doi.org/10.1016/j.envpol.2018.09.074, 2018.

Borlaza, L. J., Weber, S., Marsal, A., Uzu, G., Jacob, V., Besombes, J. L., Chatain, M., Conil, S., and Jaffrezo, J. L.: Nine-year trends of PM_{10} sources and oxidative potential in a rural background site in France, Atmos. Chem. Phys., 22, 8701–8723, https://doi.org/10.5194/acp-22-8701-2022, 2022.

Cao, J., Lee, S., Ho, K., Fung, K., Chow, J. C., and Watson, J. G.: Characterization of roadside fine particulate carbon and its eight fractions in Hong Kong, Aerosol Air Qual. Res., 6, 106–122, https://doi.org/10.4209/aaqr.2006.06.0001, 2006.

Charrier, J. G., and Anastasio, C.: On dithiothreitol (DTT) as a measure of oxidative potential for ambient particles: Evidence for the importance of soluble transition metals, Atmos. Chem. Phys., 12, 9321–9333, https://doi.org/10.5194/acp-12-9321-2012, 2012.

Chatani, S., Shimadera, H., Itahashi, S., and Yamaji, K.: Comprehensive analyses of source sensitivities and apportionments of $PM_{2.5}$ and ozone over Japan via multiple numerical techniques, Atmos. Chem. Phys., 20, 10311–10329, https://doi.org/10.5194/acp-20-10311-2020, 2020.

Cheung, R. K. Y., Qi, L., Manousakas, M. I., Puthussery, J. V., Zheng, Y., Koenig, T. K., Cui, T., Wang, T., Ge, Y., Wei, G., Kuang, Y., Sheng, M., Cheng, Z., Li, A., Li, Z., Ran, W., Xu, W., Zhang, R., Han, Y., Wang, Q., Wang, Z., Sun, Y., Cao, J., Slowik, J. G., Dällenbach, K. R., Verma, V., Gysel-Beer, M., Qiu, X., Chen, Q., Shang, J., El-Haddad, I., Prévôt, A. S. H., and Modini, R. L.: Major source categories of $PM_{2.5}$ oxidative potential in wintertime Beijing and surroundings based on online dithiothreitol-based field measurements, Sci. Total Environ., 928, 172345, https://doi.org/10.1016/j.scitotenv.2024.172345, 2024.

Cho, A. K., Sioutas, C., Miguel, A. H., Kumagai, Y., Schmitz, D. A., Singh, M., Eiguren-Fernandez, A., and Froines, J. R.: Redox activity of airborne particulate matter at different sites in the Los Angeles Basin, Environ. Res., 99, 40–47, https://doi.org/10.1016/j.envres.2005.01.003, 2005.

Chow, J. C., Watson, J. G., Pritchett, L. C., Pierson, W. R., Frazier, C. A., and Purcell, R. G.: The DRI thermal/optical reflectance carbon analysis system: Description, evaluation and applications in U.S. air quality studies, Atmos. Environ., 27, 1185–1201, https://doi.org/10.1016/0960-1686(93)90245-T, 1993.

Cohen, A. J., Brauer, M., Burnett, R., Anderson, H. R., Frostad, J., Estep, K., Balakrishnan, K., Brunekreef, B., Dandona, L., Dandona, R., Feigin, V., Freedman, G., Hubbell, B., Jobling, A., Kan, H., Knibbs, L., Liu, Y., Martin, R., Morawska, L., Pope, C. A., Shin, H., Straif, K., Shaddick, G., Thomas, M., van Dingenen, R., van Donkelaar, A., Vos, T., Murray, C. J. L., and Forouzanfar, M. H.: Estimates and 25-year trends of the global burden of disease attributable to ambient air pollution: An analysis of data from the Global Burden of Diseases Study 2015, Lancet, 389, 1907–1918, https://doi.org/10.1016/S0140-6736(17)30505-6, 2017.

Daellenbach, K. R., Uzu, G., Jiang, J., Cassagnes, L.-E., Leni, Z., Vlachou, A., Stefenelli, G., Canonaco, F., Weber, S., Segers, A., Kuenen, J. J. P., Schaap, M., Favez, O., Albinet, A., Aksoyoglu, S., Dommen, J., Baltensperger, U., Geiser, M., El Haddad, I., Jaffrezo, J.-L., and Prévôt, A. S. H.: Sources of particulate-matter air pollution and its oxidative potential in Europe, Nature, 587, 414–419, https://doi.org/10.1038/s41586-020-2902-8, 2020.

Dockery, D. W., Pope, C. A., Xu, X., Spengler, J. D., Ware, J. H., Fay, M. E., Ferris, B. G. Jr., and Speizer, F. E.: An association between air pollution and mortality in six U.S. cities, N. Engl. J. Med., 329, 1753–1759, https://doi.org/10.1056/NEJM199312093292401, 1993.

Dominutti, P. A., Borlaza, L. J. S., Sauvain, J.-J., Ngoc Thuy, V. D., Houdier, S., Suarez, G., Jaffrezo, J.-L., Tobin, S., Trébuchon, C., Socquet, S., Moussu, E., Mary, G., and Uzu, G.: Source apportionment of oxidative potential depends on the choice of the assay: insights into 5 protocols comparison and implications for mitigation measures, Environ. Sci.: Atmos., 3, 1497–1512, https://doi.org/10.1039/D3EA00007A, 2023.

Fang, Z., Lai, A., Windwer, E., Pardo, M., Li, C., Thenoor Chandran, A., Laskin, A., and Rudich, Y.: Investigating the oxidative potential and in vitro toxicity of ambient water-soluble PM_{10} in an eastern Mediterranean site, ACS ES&T Air, 2, 1326–1338, https://doi.org/10.1021/acsestair.5c00085, 2025.

Fujitani, Y., Furuyama, A., Hayashi, M., Hagino, H., and Kajino, M.: Assessing oxidative stress induction ability and oxidative potential of $PM_{2.5}$ in cities in eastern and western Japan, Chemosphere, 324, 138308, https://doi.org/10.1016/j.chemosphere.2023.138308, 2023.

Fushimi, A., Saitoh, K., Hayashi, K., Ono, K., Fujitani, Y., Villalobos, A. M., Shelton, B. R., Takami, A., Tanabe, K., and Schauer, J. J.: Chemical characterization and oxidative potential of particles emitted from open burning of cereal straws and rice husk under flaming and smoldering conditions, Atmos. Environ., 163, 118–127, https://doi.org/10.1016/j.atmosenv.2017.05.037, 2017.

Halliwell, B., and Gutteridge, J. M. C.: Free Radicals in Biology and Medicine, Oxford University Press, Oxford, UK, https://doi.org/10.1093/acprof:oso/9780198717478.001.0001, 2015.

Han, Y., Cao, J., Chow, J. C., Watson, J. G., An, Z., Jin, Z., Fung, K., and Liu, S.: Evaluation of the thermal/optical reflectance method for discrimination between char- and soot-EC, Chemosphere, 69, 569–574, https://doi.org/10.1016/j.chemosphere.2007.03.024, 2007.

Hara, K., Takashima, H., Yoshino, A., Takami, A., Nishita-Hara, C., Fujiyoshi, Y., and Hayashi, M.: Seasonal variations of diurnal cycles of aerosols and gases in the Fukuoka Plain, Japan: Effects of local meteorology and atmospheric chemistry, Atmos. Environ., 289, 119318, https://doi.org/10.1016/j.atmosenv.2022.119318, 2022.

Hoek, G., Krishnan, R. M., Beelen, R., Peters, A., Ostro, B., Brunekreef, B., and Kaufman, J. D.: Long-term air pollution exposure and cardio-respiratory mortality: A review, Environ. Health, 12, 43, https://doi.org/10.1186/1476-069X-12-43, 2013.

Honda, A., Okuda, T., Nagao, M., Miyasaka, N., Tanaka, M., and Takano, H.: PM2.5 collected using cyclonic separation causes stronger biological responses than that collected using a conventional filtration method, Environ. Res., 198, 110490, https://doi.org/10.1016/j.envres.2020.110490, 2021.

Honda, A., Inoue, K. I., Higashihara, M., Ichinose, T., Ueda, K., and Takano, H.: Differential pattern of cell death and ROS production in human airway epithelial cells exposed to quinones combined with heated-PM2.5 and/or Asian sand dust, Int. J. Mol. Sci., 24, 10544, https://doi.org/10.3390/ijms241310544, 2023.

Hu, S., Polidori, A., Arhami, M., Shafer, M. M., Schauer, J. J., Cho, A., and Sioutas, C.: Redox activity and chemical speciation of size fractioned PM in the communities of the Los Angeles – Long Beach harbor, Atmos. Chem. Phys., 8, 6439–6451, https://doi.org/10.5194/acp-8-6439-2008, 2008.

Iijima, A., Sato, K., Fujitani, Y., Fujimori, E., Saito, Y., Tanabe, K., Ohara, T., Kozawa, K., and Furuta, N.: Clarification of the predominant emission sources of antimony in airborne particulate matter and estimation of their effects on the atmosphere in Japan, Environ. Chem., 6, 122–132, https://doi.org/10.1071/EN08107, 2009.

Itahashi, S., Uno, I., and Kim, S.: Source contributions of sulfate aerosol over East Asia estimated by CMAQ-DDM, Environ. Sci. Technol., 46, 6733–6741, https://doi.org/10.1021/es300887w, 2012.

Iwamoto, Y., Kinouchi, K., Watanabe, K., Yamazaki, N., and Matsuki, A.: Simultaneous measurement of CCN activity and chemical composition of fine-mode aerosols at Noto Peninsula, Japan, in autumn 2012, Aerosol Air Qual. Res., 16, 2107–2118, https://doi.org/10.4209/aaqr.2015.09.0545, 2016.

Jiang, H. H., Ahmed, C. M. S., Canchola, A., Chen, J. Y., and Lin, Y. H.: Use of dithiothreitol assay to evaluate the oxidative potential of atmospheric aerosols, Atmosphere, 10, 571, https://doi.org/10.3390/atmos10100571, 2019.

Jin, S., Yoon, S.-J., Jung, N.-Y., Lee, W. S., Jeong, J., Park, Y.-J., Kim, W., Oh, D.-B., and Seo, J.: Antioxidants prevent particulate matter-induced senescence of lung fibroblasts, Heliyon, 9, e14179, https://doi.org/10.1016/j.heliyon.2023.e14179, 2023.

Kalyanaraman, B., Darley-Usmar, V., Davies, K. J. A., Dennery, P. A., Forman, H. J., Grisham, M. B., Mann, G. E., Moore, K., Roberts, L. J., and Ischiropoulos, H.: Measuring reactive oxygen and nitrogen species with fluorescent probes: challenges and limitations, Free Radic. Biol. Med., 52, 1–6, https://doi.org/10.1016/j.freeradbiomed.2011.09.030, 2012.

Kaneyasu, N., Yamamoto, S., Sato, K., Takami, A., Hayashi, M., Hara, K., Kawamoto, K., Okuda, T., and Hatakeyama, S.: Impact of long-range transport of aerosols on the $PM_{2.5}$ composition at a major metropolitan area in the northern Kyushu area of Japan, Atmos. Environ., 97, 416–425, https://doi.org/10.1016/j.atmosenv.2014.01.029, 2014.

Kim, P.-R., Park, S.-W., Han, Y.-J., Lee, M.-H., Holsen, T. M., Jeong, C.-H., and Evans, G.: Variations of oxidative potential of $PM_{2.5}$ in a medium-sized residential city in South Korea measured using three different chemical assays, Sci. Total Environ., 920, 171053, https://doi.org/10.1016/j.scitotenv.2024.171053, 2024.

Koo, J.-H., Park, S.-W., Lee, H.-W., Kim, P.-R., Jeon, J.-W., Kwak, K.-H., Yi, S.-M., Collett, J. L., and Han, Y.-J.: Quantitative analysis of $PM_{2.5}$ oxidative potential: Insights into the role of organic compounds and sources, J. Hazard. Mater., 497, 139707, https://doi.org/10.1016/j.jhazmat.2025.139707, 2025.

Kumagai, Y., Koide, S., Taguchi, K., Endo, A., Nakai, Y., Yoshikawa, T., and Shimojo, N.: Oxidation of proximal protein sulfhydryls by phenanthraquinone, a component of diesel exhaust particles, Chem. Res. Toxicol., 15, 483–489, https://doi.org/10.1021/tx0100993, 2002.

Kurihara, K., Iwata, A., Murray Horwitz, S. G., Ogane, K., Sugioka, T., Matsuki, A., and Okuda, T.: Contribution of physical and chemical properties to dithiothreitol-measured oxidative potentials of atmospheric aerosol particles at urban and rural sites in Japan, Atmosphere, 13, 319, https://doi.org/10.3390/atmos13020319, 2022.

Laden, F., Schwartz, J., Speizer, F. E., and Dockery, D. W.: Reduction in fine particulate air pollution and mortality, Am. J. Respir. Crit. Care Med., 173, 667–672, https://doi.org/10.1164/rccm.200503-443OC, 2006.

Landreman, A. P., Shafer, M. M., Hemming, J. C., Hannigan, M. P., and Schauer, J. J.: A Macrophage-Based Method for the Assessment of the Reactive Oxygen Species (ROS) Activity of Atmospheric Particulate Matter (PM) and Application to Routine (Daily 24 h) Aerosol Monitoring Studies, Aerosol Sci Tech, 42, 946–957, https://doi.org/10.1080/02786820802363819, 2008.

Lelieveld, J., Evans, J. S., Fnais, M., Giannadaki, D., and Pozzer, A.: The contribution of outdoor air pollution sources to premature mortality on a global scale, Nature, 525, 367–371, https://doi.org/10.1038/nature15371, 2015.

Li, N., Sioutas, C., Cho, A., Schmitz, D., Misra, C., Sempf, J., Wang, M., Oberley, T., Froines, J., and Nel, A.: Ultrafine particulate pollutants induce oxidative stress and mitochondrial damage, Environ. Health Perspect., 111, 455–460, https://doi.org/10.1289/ehp.6000, 2003.

Li, Q., Wyatt, A., and Kamens, R. M.: Oxidant generation and toxicity enhancement of aged-diesel exhaust, Atmos. Environ., 43, 1037–1042, https://doi.org/10.1016/j.atmosenv.2008.11.018, 2009.

Lin, P., and Yu, J. Z.: Generation of reactive oxygen species mediated by humic-like substances in atmospheric aerosols, Environ. Sci. Technol., 45, 10362–10368, https://doi.org/10.1021/es2028229, 2011.

Lin, M. F., and Yu, J. Z.: Dithiothreitol (DTT) concentration effect and its implications on the applicability of DTT assay to evaluate the oxidative potential of atmospheric aerosol samples, Environ. Pollut., 251, 938–944, https://doi.org/10.1016/j.envpol.2019.05.074, 2019.

Liu, F., Saavedra, M. G., Champion, J. A., Griendling, K. K., and Ng, N. L.: Prominent contribution of hydrogen peroxide to intracellular reactive oxygen species generated upon exposure to naphthalene secondary organic aerosols, Environ. Sci. Technol. Lett., 7, 171–177, https://doi.org/10.1021/acs.estlett.9b00773, 2020a.

Liu, Q., Lu, Z., Xiong, Y., Huang, F., Zhou, J., and Schauer, J. J.: Oxidative potential of ambient $PM_{2.5}$ in Wuhan and its comparisons with eight areas of China, Sci. Total Environ., 701, 134844, https://doi.org/10.1016/j.scitotenv.2019.134844, 2020b.

Liu, F., Joo, T., Ditto, J. C., Saavedra, M. G., Takeuchi, M., Boris, A. J., Yang, Y., Weber, R. J., Dillner, A. M., Gentner, D. R., and Ng, N. L.: Oxidized and unsaturated: Key organic aerosol traits associated with cellular reactive oxygen species production in the southeastern United States, Environ. Sci. Technol., 57, 14150–14161, https://doi.org/10.1021/acs.est.3c03641, 2023.

Michael, S., Montag, M., and Dott, W.: Pro-inflammatory effects and oxidative stress in lung macrophages and epithelial cells induced by ambient particulate matter, Environ. Pollut., 183, 19–29, https://doi.org/10.1016/j.envpol.2013.01.026, 2013.

Michikawa, T., Ueda, K., Takami, A., Sugata, S., Yoshino, A., Nitta, H., and Yamazaki, S.: Japanese nationwide study on the association between short-term exposure to particulate matter and mortality, J. Epidemiol., 29, 471–477, https://doi.org/10.2188/jea.JE20180122, 2019.

Molina, C., Toro, A. R., Manzano, C. A., Canepari, S., Massimi, L., and Leiva-Guzmán, M. A.: Airborne aerosols and human health: Leapfrogging from mass concentration to oxidative potential, Atmosphere, 11, 917, https://doi.org/10.3390/atmos11090917, 2020.

Murphy, M. P., Bayir, H., Belousov, V., Chang, C. J., Davies, K. J. A., Davies, M. J., Dick, T. P., Finkel, T., Forman, H. J., Janssen-Heininger, Y., Gems, D., Kagan, V. E., Kalyanaraman, B., Larsson, N.-G., Milne, G. L., Nyström, T., Poulsen, H. E., Radi, R., Van Remmen, H., Schumacker, P. T., Thornalley, P. J., Toyokuni, S., Winterbourn, C. C., Yin, H., and Halliwell, B.: Guidelines for measuring reactive oxygen species and oxidative damage in cells and in vivo, Nat. Metab., 4, 651–662, https://doi.org/10.1038/s42255-022-00591-z, 2022.

Nel, A.: Air pollution-related illness: Effects of particles, Science, 308, 804–806, https://doi.org/10.1126/science.1108752, 2005.

Nicolas, J., Jaafar, M., Sepetdjian, E., Saad, W., Sioutas, C., Shihadeh, A., and Saliba, N. A.: Redox activity and chemical interactions of metal oxide nano- and micro-particles with dithiothreitol (DTT), Environ. Sci.: Process. Impacts, 17, 1952–1958, https://doi.org/10.1039/c5em00352k, 2015.

Nishita-Hara, C., Hirabayashi, M., Hara, K., Yamazaki, A., and Hayashi, M.: Dithiothreitol-measured oxidative potential of size-segregated particulate matter in Fukuoka, Japan: Effects of Asian dust events, GeoHealth, 3, 160–173, https://doi.org/10.1029/2019GH000189, 2019.

Nishita-Hara, C., Kobayashi, H., Hara, K., and Hayashi, M.: Dithiothreitol-measured oxidative potential of reference materials of mineral dust: Implications for the toxicity of mineral dust aerosols in the atmosphere, GeoHealth, 7, e2022GH000736, https://doi.org/10.1029/2022GH000736, 2023.

Nishita-Hara, C., Nakano, K., Iwata, A., bin Mohd Nor, M. A., Mori, T., Youn, H., and Okuda, T.: Development of an openable small cyclone for atmospheric particulate matter sampling for toxicological experiments, Aerosol Sci. Technol., 1–13, https://doi.org/10.1080/02786826.2024.2322680, 2024.

Okuda, T., Kato, J., Mori, J., Tenmoku, M., Suda, Y., Tanaka, S., He, K., Ma, Y., Yang, F., Yu, X., Duan, F., and Lei, Y.: Daily concentrations of trace metals in aerosols in Beijing, China, determined by using inductively coupled plasma mass spectrometry equipped with laser ablation analysis, and source identification of aerosols, Sci. Total Environ., 330, 145–158, https://doi.org/10.1016/j.scitotenv.2004.04.010, 2004.

Okuda, T.: Measurement of the specific surface area and particle size distribution of atmospheric aerosol reference materials, Atmos. Environ., 75, 1–5, https://doi.org/10.1016/j.atmosenv.2013.04.033, 2013.

Onishi, T., Honda, A., Tanaka, M., Chowdhury, P. H., Okano, H., Okuda, T., Shishido, D., Terui, Y., Hasegawa, S., Kameda, T., Tohno, S., Hayashi, M., Nishita-Hara, C., Hara, K., Inoue, K., Yasuda, M., Hirano, S., and Takano, H.: Ambient fine and coarse particles in Japan affect nasal and bronchial epithelial cells differently and elicit varying immune response, Environ. Pollut., 242, 1693–1701, https://doi.org/10.1016/j.envpol.2018.07.103, 2018.

Park, J., Park, E. H., Schauer, J. J., Yi, S. M., and Heo, J.: Reactive oxygen species (ROS) activity of ambient fine particles ($PM_{2.5}$) measured in Seoul, Korea, Environ. Int., 117, 276-283, https://doi.org/10.1016/j.envint.2018.05.018, 2018a.

Park, M., Joo, H. S., Lee, K., Jang, M., Kim, S. D., Kim, I., Borlaza, L. J. S., Lim, H., Shin, H., Chung, K. H., Choi, Y.-H., Park, S. G., Bae, M.-S., Lee, J., Song, H., and Park, K.: Differential toxicities of fine particulate matters from various sources, Sci. Rep., 8, 17007, https://doi.org/10.1038/s41598-018-35398-0, 2018b.

Penning, T. M., Burczynski, M. E., Hung, C.-F., McCoull, K. D., Palackal, N. T., and Tsuruda, L. S.: Dihydrodiol dehydrogenases and polycyclic aromatic hydrocarbon activation: Generation of reactive and redox active o-quinones, Chem. Res. Toxicol., 12, 1–18, https://doi.org/10.1021/tx980143n, 1999.

Pope III, C. A., Burnett, R. T., Thun, M. J., Calle, E. E., Krewski, D., Ito, K., and Thurston, G. D.: Lung cancer, cardiopulmonary mortality, and long-term exposure to fine particulate air pollution, J. Am. Med. Assoc., 287, 1132–1141, https://doi.org/10.1001/jama.287.9.1132, 2002.

Seinfeld, J. H., and Pandis, S. N.: Atmospheric Chemistry and Physics: From Air Pollution to Climate Change, John Wiley & Sons, Hoboken, NJ, USA, 2016.

Shimada, K., Mizukoshi, M., Chan, C. K., Kim, Y. P., Lin, N.-H., Matsuda, K., Itahashi, S., Nakashima, Y., Kato, S., and Hatakeyama, S.: Disentangling the contribution of the transboundary out-flow from the Asian continent to Tokyo, Japan, Environ. Pollut., 286, 117280, https://doi.org/10.1016/j.envpol.2021.117280, 2021.

Shiraiwa, M., Ueda, K., Pozzer, A., Lammel, G., Kampf, C. J., Fushimi, A., Enami, S., Arangio, A. M., Frohlich-Nowoisky, J., Fujitani, Y., Furuyama, A., Lakey, P. S. J., Lelieveld, J., Lucas, K., Morino, Y., Pöschl, U., Takahama, S., Takami, A., Tong, H., Weber, B., Yoshino, A., and Sato, K.: Aerosol health effects from molecular to global scales, Environ. Sci. Technol., 51, 13545–13567, https://doi.org/10.1021/acs.est.7b04417, 2017.

Stein, A. F., Draxler, R. R., Rolph, G. D., Stunder, B. J. B., Cohen, M. D., and Ngan, F.: NOAA's HYSPLIT atmospheric transport and dispersion modeling system, Bull. Am. Meteorol. Soc., 96, 2059–2077, https://doi.org/10.1175/BAMS-D-14-00110.1, 2015.

Thermo Fisher Scientific: The Molecular Probes® Handbook: A guide to fluorescent probes and labeling technologies, Available at: https://www.thermofisher.com/jp/en/home/references/molecular-probes-the-handbook.html (last access: 25 June 2025), 2025.

Venkatachari, P., Hopke, P. K., Grover, B. D., and Eatough, D. J.: Measurement of particle-bound reactive oxygen species in Rubidoux aerosols, J. Atmos. Chem., 50, 49–58, https://doi.org/10.1007/s10874-005-1662-z, 2005.

Verma, V., Polidori, A., Schauer, J. J., Shafer, M. M., Cassee, F. R., and Sioutas, C.: Physicochemical and toxicological profiles of particulate matter in Los Angeles during the October 2007 Southern California wildfires, Environ. Sci. Technol., 43, 954–960, https://doi.org/10.1021/es8021667, 2009.

Verma, V., Rico-Martinez, R., Kotra, N., King, L., Liu, J., Snell, T. W., and Weber, R. J.: Contribution of water-soluble and insoluble components and their hydrophobic/hydrophilic subfractions to the reactive oxygen species-generating potential of fine ambient aerosols, Environ. Sci. Technol., 46, 11384–11392, https://doi.org/10.1021/es302484r, 2012.

Verma, V., Fang, T., Xu, L., Peltier, R. E., Russell, A. G., Ng, N. L., and Weber, R. J.: Organic aerosols associated with the generation of reactive oxygen species (ROS) by water-soluble $PM_{2.5}$, Environ. Sci. Technol., 49, 4646–4656, https://doi.org/10.1021/es505577w, 2015.

Wang, Q. and Li, R.: Journey to burning half of global coal: Trajectory and drivers of China′s coal use, Renewable and Sustainable Energy Reviews, 58, 341-346, https://doi.org/10.1016/j.rser.2015.12.104, 2016.

Wang, Y., Wang, M., Li, S., Sun, H., Mu, Z., Zhang, L., Li, Y., and Chen, Q.: Study on the oxidation potential of the water-soluble components of ambient $PM_{2.5}$ over Xi'an, China: Pollution levels, source apportionment and transport pathways, Environ. Int., 136, 105515, https://doi.org/10.1016/j.envint.2020.105515, 2020.

Weber, S., Uzu, G., Favez, O., Borlaza, L. J. S., Calas, A., Salameh, D., Chevrier, F., Allard, J., Besombes, J. L., Albinet, A., Pontet, S., Mesbah, B., Gille, G., Zhang, S., Pallares, C., Leoz-Garziandia, E., and Jaffrezo, J. L.: Source apportionment of atmospheric PM_{10} oxidative potential: synthesis of 15 year-round urban datasets in France, Atmos. Chem. Phys., 21, 11353–11378, https://doi.org/10.5194/acp-21-11353-2021, 2021.

Xia, T., Kovochich, M., Brant, J., Hotze, M., Sempf, J., Oberley, T., Sioutas, C., Yeh, J. I., Wiesner, M. R., and Nel, A. E.: Comparison of the abilities of ambient and manufactured nanoparticles to induce cellular toxicity according to an oxidative stress paradigm, Nano Lett., 6, 1794–1807, https://doi.org/10.1021/nl061025k, 2006.

Xing, C., Wang, Y., Yang, X., Zeng, Y., Zhai, J., Cai, B., Zhang, A., Fu, T. M., Zhu, L., Li, Y., Wang, X., and Zhang, Y.: Seasonal variation of driving factors of ambient $PM_{2.5}$ oxidative potential in Shenzhen, China, Sci. Total Environ., 862, 160771, https://doi.org/10.1016/j.scitotenv.2022.160771, 2023.

Xiong, Q. S., Yu, H. R., Wang, R. R., Wei, J. L., and Verma, V.: Rethinking dithiothreitol-based particulate matter oxidative potential: Measuring dithiothreitol consumption versus reactive oxygen species generation, Environ. Sci. Technol., 51, 6507–6514, https://doi.org/10.1021/acs.est.7b01272, 2017.

Yim, S. H. L., Gu, Y., Shapiro, M. A., and Stephens, B.: Air quality and acid deposition impacts of local emissions and transboundary air pollution in Japan and South Korea, Atmos. Chem. Phys., 19, 13309–13323, https://doi.org/10.5194/acp-19-13309-2019, 2019.

Yoshino, A., Takami, A., Hara, K., Nishita-Hara, C., Hayashi, M., and Kaneyasu, N.: Contribution of local and transboundary air pollution to the urban air quality of Fukuoka, Japan, Atmosphere, 12, 431, https://doi.org/10.3390/atmos12040431, 2021.

Yu, J., Yan, C., Liu, Y., Li, X., Zhou, T., and Zheng, M.: Potassium: a tracer for biomass burning in Beijing?, Aerosol Air Qual. Res., 18, 2447–2459, https://doi.org/10.4209/aaqr.2017.11.0536, 2018.

Yu, S., Liu, W., Xu, Y., Yi, K., Zhou, M., Tao, S., and Liu, W.: Characteristics and oxidative potential of atmospheric $PM_{2.5}$ in Beijing: Source apportionment and seasonal variation, Sci. Total Environ., 650, 277–287, https://doi.org/10.1016/j.scitotenv.2018.09.021, 2019.

Zhang, Y. L., Huang, R. J., El Haddad, I., Ho, K. F., Cao, J. J., Han, Y., Zotter, P., Bozzetti, C., Daellenbach, K. R., Canonaco, F., Slowik, J. G., Salazar, G., Schwikowski, M., Schnelle-Kreis, J., Abbaszade, G., Zimmermann, R., Baltensperger, U., Prévôt, A. S. H., and Szidat, S.: Fossil vs. non-fossil sources of fine carbonaceous aerosols in four Chinese cities during the extreme winter haze episode of 2013, Atmos. Chem. Phys., 15, 1299–1312, https://doi.org/10.5194/acp-15-1299-2015, 2015.